Electron-Attachment Reactions in Molecular Clusters

Eugen Illenberger

Institut für Physikalische und Theoretische Chemie, Freie Universität Berlin, Takustrasse 3, D-1000 Berlin 33

Contents

I. Introduction

Low-energy electrons can be very reactive in that they are effectively captured by many molecules which then undergo rapid unimolecular decompositions. The cross section for such processes can be very large, several orders of magnitude larger than ionization or excitation cross sections.[1,2] Electron-attachment reactions to molecules in the gas phase have been studied to some extent within the last two or three decades. Analogous experiments in clusters, on the other hand, have only recently been performed.

This contribution focuses on reactions in weakly bound van der Waals clusters induced by low-energy (0–10 eV) electron capture. Particular emphasis will be placed on the question how the basic quantities of such processes (i.e. attachment energy, evolution of the negatively charged compound, and energy distribution of the products ultimately formed) behave on proceeding from an isolated molecule under single collision conditions to a molecular aggregate.

Eugen Illenberger studied Physics at the Universities of Heidelberg and Freiburg (Germany) and received his Diplom (1972) and Dr. rer. nat. Degree (1976) under A. Niehaus in Molecular Physics (Penning Electron Spectroscopy). He then moved to the Free University (Berlin), where he habilitated (1983) in Physical Chemistry (Negative Ions in the Gas Phase). After a year at the Chemistry Department at Stanford University, he returned to the Free University where he has now been a Professor since 1989. His research interests are directed to gas-phase ion chemistry and the behavior of electrons and ions in condensed matter.

During the past decade there has been an enormous increase of experimental and theoretical work concerning the properties of clusters.[3–10] Since the term "cluster" is frequently used with different meanings, we will in the context of this contribution assign a group of molecules in the gas phase which are held together by weak intermolecular forces as a molecular cluster or a molecular aggregate. In that sense, a free molecular cluster can be viewed as representing a link between molecules in the gas phase and in the condensed phase (bulk liquids or solids).

Traditionally, science has concentrated on understanding these two separate forms of matter and only recently fundamental questions such as the minimum number of atoms necessary to evolve an electric conduction band or the number of atoms or molecules required to support a bulk crystal structure have emerged.

Electron-attachment and -detachment processes or, more generally, electron-transfer reactions play a key role in many fields of pure and applied science, in the gas phase (discharges, gaseous dielectrics, atmospheric processes, etc.) as well as in the condensed phase (electrochemistry, biochemical systems, etc.). Within these different fields the general area of noncovalent van der Waals interactions between molecules and their behavior when they are subjected to excitation or ionization plays a central role in many fields of present-day natural science.

Negatively charged clusters are of particular interest since they are considered to provide models for excess

electrons in liquids.[3,4,33,34] Apart from this, as we will demonstrate, the study of electron-attachment reactions in homogeneous and heterogeneous clusters allows insight into very fundamental properties like electronic states of molecular ions, selection rules to populate them, as well as intra- and intermolecular energy and electron-transfer processes.

Before considering electron capture by molecular clusters, we will briefly recall some important facts on negative ions.

The *basic quantity* in the relation of a neutral particle (M) with its negative ion (M⁻) is the *electron affinity*. The *adiabatic electron affinity* of a particle is formally defined as the energy difference between the neutral and the anion in their respective ground states. By convention, the electron affinity of M is considered *positive* if the ground state of M⁻ lies *below* that of M, and *negative* if M⁻ lies *above* the neutral molecule M. A positive value for the electron affinity indicates the existence of a stable anion in which the extra electron exists in a (thermodynamically) bound state.

In molecules which are characterized by considerable geometry changes between the anion and the neutral, we have to distinguish between the adiabatic electron affinity (EA) of M and the vertical detachment energy (VDE) of M⁻. The latter is the number which is experimentally obtained in a Franck–Condon transition in photodetachment from molecular anions, in complete analogy to adiabatic and vertical ionization energies in photoionization. In systems where the geometry change is not too large, optical photodetachment does directly allow to measure the adiabatic electron affinity.[11,12]

In the gas phase under single collision conditions a stable molecular anion M⁻ can, for instance, be generated by electron transfer from neutrals or anions[13,14] according to

$$A + M \rightarrow A^+ + M^- \tag{1}$$

$$A^- + M \rightarrow A + M^- \tag{2}$$

Since the binding energy of the extra electron to M⁻ is usually less than the ionization energy of A, reaction 1 is generally endothermic and can only occur if A and M contain sufficient (translational/internal) energy.

This contribution deals with reactions induced in molecular aggregates following capture of *free* electrons.

Consider first an isolated molecule in the gas phase interacting with electrons of defined but variable energy. This interaction is commonly divided into two major classes, *direct* and *resonance* scattering.[2,15–18] In the first case, the electron collides with the target molecule and will be deviated from its original direction. If the scattering process is inelastic, the electron will lose some of its initial energy thereby leaving the target molecule in an excited state. Resonant scattering is considered to occur when the incoming electron is temporarily trapped in a potential created by its interaction with the neutral molecule thus forming a *temporary negative ion* (TNI):

$$e^- + M \rightarrow M^{-(*)} \tag{3}$$

Synonymously, the molecular anion is called a *resonance* since its formation represents an electronic transition from a continuum state (M + e⁻) to a discrete

state (M⁻⁽*⁾). Note that free-electron capture is an electronic transition which, in any case, initially creates an unstable (or metastable) negative ion with respect to ejection of the extra electron. If by that the *ground state* of the anion is formed, M possesses a *negative* electron affinity, since the energy of the anion is *above* that of the neutral.
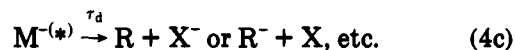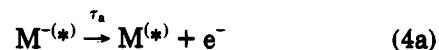
Of course, low-energy electron attachment can also lead to excited states of the anion. SF₆, for example, captures electrons near 0 eV to form the anion in its electronic ground state, but vibrationally excited.[1,2,28]

At this point we will not discuss the classification and genealogy of resonances to any great extent, but rather refer the reader to some relevant review articles.[15–21] For the purpose of this contribution it is sufficient to distinguish between *single particle* (1p) and *two particle–one hole* (2p-1h) resonances. In the first case, the incoming electron temporarily occupies one of the normally empty (or virtual) MOs without affecting the configuration of the other electrons.

The trapping mechanism is described by the *shape* of the interaction potential between the electron and the neutral molecule: combination of the attractive polarization interaction ($-\alpha e^2/2r^4$; α, polarizability of the target molecule) and the repulsive centrifugal term ($\hbar^2 l(l + l)/2\mu r^2$; l, angular momentum quantum number of the incoming electron; μ, reduced mass of the electron and the target molecule) results in a centrifugal barrier in the effective potential in which the additional electron can temporarily be trapped. Since it is the particular shape of the potential which is responsible for the trapping, these states are also called *shape resonances*.

A two particle–one hole (2p-1h) resonance is formed when the incoming electron concomitantly excites one of the electrons of the target molecule resulting in one hole and two electrons in normally unfilled MOs. This is analogous to the formation of 1p-2h (non-Koopmans') states in positive ions.[22,23] If the energy of the core excited resonance lies *below* that of the associated excited neutral state, the extra electron is simply trapped in the field of the excited molecule (Feshbach resonance); if it lies *above*, again the *shape* of the interaction potential is responsible for the trapping and we speak of a *core-excited shape resonance*.

Under *single collision conditions*, the principal decomposition processes of such resonances are

$$M^{-(*)} \xrightarrow{\tau_a} M^{(*)} + e^- \tag{4a}$$

$$M^{-(*)} \xrightarrow{\tau_r} M^- + \hbar\omega \tag{4b}$$

$$M^{-(*)} \xrightarrow{\tau_d} R + X^- \text{ or } R^- + X, \text{ etc.} \tag{4c}$$

Channel 4a is autodetachment, often associated with vibrational excitation of the neutral molecule, reaction 4b is radiative stabilization to the thermodynamically stable ground state which is possible for molecules possessing a positive electron affinity, and reaction 4c represents unimolecular decomposition into stable negative and neutral fragments (dissociative attachment).

The autodetachment lifetime τ_a varies over a wide scale, depending on the energy of the resonance and

the size of the molecule and ranges from less than a vibrational period (10^{-14} s) to the micro- or millisecond scale for larger molecules such as SF_6 or polycyclic aromatic hydrocarbons.[24-29] These metastable anion states are typically generated within a narrow resonance near 0 eV where dissociation channels 4c are not yet accessible.
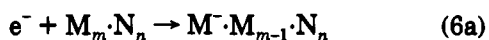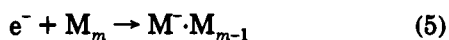
Data concerning radiative stabilization are scarce for molecules. With radiative lifetimes of the order of 10^{-9}–10^{-8} s it is indeed likely that channel 4b is slow compared with the competing reactions 4a and 4c. However, in the case of long-lived anions formed near 0 eV (like SF_6^{*-} mentioned above which cannot decay by dissociation) radiative cooling was discussed as an effective mechanism to form stable anions in ICR experiments.[30,31]

Finally, channel 4c (dissociative electron attachment) typically occurs on a time scale ranging between 10^{-14} and 10^{-12} s, depending on the *mechanism* of the reaction (direct electronic dissociation along a repulsive potential energy surface or more indirect processes such as electronic or vibrational predissociation). Reaction 4c can occur if (a) thermodynamically stable, negatively charged fragments exist for the respective compound and (b) these channels are energetically available at the energy of the TNI.

How does the situation change when an isolated molecule M under single collision conditions is replaced by a homogeneous molecular cluster M_m or a heterogeneous cluster $M_m \cdot N_n$?

In terms of molecular orbitals (MOs) electron capture by molecules is considered to occur via accommodation of the excess electron into a normally unfilled MO. This is no longer necessarily the case in clusters or in the condensed phase. Water clusters, e.g., can capture low-energy electrons to form $(H_2O)_n^-$, $n \geq 11$ as demonstrated by Echt, Recknagel, and co-workers.[32] The electronically and geometrically relaxed compound (at least for larger clusters) can be pictured by trapping of the excess electron in the field of the oriented water dipoles.[33-35] Solvated electrons have been well known to exist in polar liquids for more than 100 years.[36]

As we shall demonstrate, negative-ion formation in low-energy electron impact to clusters can proceed via two different schemes: (i) in the primary step the incoming electron is captured to form a *localized anion* within the homogeneous or heterogeneous aggregate

$$e^- + M_m \rightarrow M^- \cdot M_{m-1} \tag{5}$$

$$e^- + M_m \cdot N_n \rightarrow M^- \cdot M_{m-1} \cdot N_n \tag{6a}$$

$$\rightarrow N^- \cdot N_{n-1} \cdot M_m \tag{6b}$$

followed by more or less complex decomposition processes involving inter- and intramolecular charge and energy transfer; (ii) in the primary step the incoming electron is *inelastically* scattered in the cluster and the slowed down electron is captured by another molecule in the second step.

The following substantial questions then arise:

1. The electronic states populated by electron capture are controlled by certain symmetry rules.[37] Are these selection rules which hold in the single molecule-

electron frame of reference violated in clusters as it is sometimes observed in the condensed phase?

2. Does a cluster environment provide the proper medium to carry off excess energy necessary to prepare thermodynamically stable molecular anions in their relaxed configuration, not accessible under isolated conditions (collisional stabilization instead of the slow radiative stabilization 4b)?

3. Which are the products ultimately formed? The possible decomposition of an ionized complex may schematically be expressed as

$$(M_m \cdot N_n)^- \rightarrow N^- + N_{n-1} \cdot M_m \tag{7a}$$

$$\rightarrow R_1^- + R_2 \tag{7b}$$
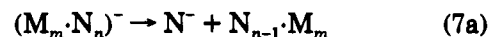
The point is then to record the *resonance profiles* of the different product ions, i.e., their formation probability as function of the initial electron energy. It must be emphasized that the energy profile of any product ion reflects the primary step of electron capture, regardless of the mechanism and complexity of its formation process. In other words, the ion yield curve of any product reflects the "electron absorption" profile of the target from which it is formed. This is true as long as the anion is formed in the primary step, i.e. inelastic scattering processes (secondary reactions) can be neglected.

4. Many dissociative attachment reactions are known to proceed directly along repulsive potential energy surfaces and hence via the release of considerable amounts of excess translational energy.[2,38-40] How does the distribution of excess energy change when the repulsive TNI is formed within a cluster?

To date experiments on attachment of free electrons of variable energy to clusters have been reported by five groups (Oak Ridge,[41-46] Innsbruck,[47-57] Konstanz,[32,58-61,157] Nowosibirsk,[62,63] and Berlin[2,38,64-71,121,125]). These investigations included clusters of O_2, CO_2, H_2O, N_2O, SO_2, SF_6, CF_4, C_2F_4, C_2F_6, C_2F_3Cl, and CH_3CN. In all these experiments free electrons of (more or less) defined energy are attached to preexisting clusters produced by supersonic expansion through a nozzle.

It has been demonstrated that both the mode of interaction of the electron with the target and the processes induced by the excess charge may substantially change on going from the monomer to clusters.

In clusters composed of molecules with positive EA the availability of collision partners in the cluster lead to the observation of stabilized anions, including the monomer. Systems belonging to this type are O_2,[48,49,71,121] SO_2,[52] N_2O,[59,60] and a number of halocarbons.[69,157]

On the other hand for molecules possessing a negative EA the value may even change to positive values in clusters. The CO_2 molecule, e.g., has an EA of −0.6 eV and is thus unstable with respect to autodetachment. By contrast, formation of negative ions following electron attachment to CO_2 clusters revealed $(CO_2)_n^-$ ions with $n > 2$ which seemed completely stable with respect to autodetachment.[42,45] Furthermore, the $(CO_2^-) \cdot H_2O$ ion formed from mixed clusters was also found to be stable.[45,46] It thus appears that solvation by a single molecule can have a significant effect on the electron affinity.

In more detailed studies it was explicitely shown that in addition to the 3-eV resonance known from the CO_2 monomer, clusters exhibit an additional resonance near 0 eV.[56,157] Johnson et al.[72] analyzed photoelectron spectra of negatively charged CO_2 clusters and suggested that the dimer ion is the core of clusters $2 < n < 5$ while the monomer ion forms the core for $n > 7$.

Finally, Echt, Recknagel and co-workers[32] succeeded to observe $(H_2O)_n^-$, $n > 11$ by attachment of near-zero energy electrons to preexisting water clusters. It has been shown before by Haberland et al.[73-76] that solvated ions of the form $(H_2O)_n^-$ and $(NH_3)_n^-$ can readily be formed in supersonic beams.

In that experiment negative cluster ions were formed following electron impact in the expansion zone of a supersonic beam. This method was extensively applied (and developed) by Haberland et al.[34] to study the minimal number of H_2O and NH_3 molecules or Xe atoms necessary to support a bound state for an excess electron. All these systems can probably not form stable negative ions as isolated particles. The minimal numbers were found to be $n = 2$ for $(H_2O)_n^-$,[73-75] $n = 35$ for $(NH_3)_n^-$,[76,77] and $n = 1$ in the case of Xe_n^-.[78] However, for Xe^- it is not yet clear whether the detected species is really associated with ground state Xe (which would indicate a positive electron affinity) or whether it represents an electronically excited (metastable) Xe^{*-} ion. In the meantime photoelectron spectra of hydrated electron cluster anions $(H_2O)_n^-$, $n = 2-69$ have been recorded by Bowen, Haberland, and co-workers.[35] It has been shown that the vertical detachment energy increases continuously from near 0 eV ($n = 2$) to 2 eV ($n = 69$). Although these experiments are in qualitative agreement with the quantum path integral molecular dynamics simulations performed by Landman and co-workers[79-82] there is no indication of a transition from a surface state to an internal state in the region between 32 and 64 as predicted by the calculations.

We here mention a further method important in that field namely electron transfer from highly excited atoms to electronegative molecules. In this technique rare gas atoms in Rydberg states were either generated by electron impact (Kondow et al.[83-85] or prepared state selectively into defined quantum numbers (nl) via laser excitation from the metastable intermediate state (Hotop et al.,[86-88] Desfrancois et al.[89,90]). In the case of $(N_2O)_n$ and $(CF_3Cl)_n$ a surprisingly strong dependence from the principle quantum number for the resulting negative ion spectra was observed.[87] In the case of water clusters[90] the dimer anion showed a particularly strong signal in the transfer reaction from Xe^* ($n = 12$), corresponding to a Rydberg mean energy of 95 meV.

The present contribution focuses on reactions in homogeneous and heterogeneous van der Waals clusters induced by attachment of *free* electrons in the range between 0 and 15 eV. Such reactions often occur at very low energies, sometimes near 0 eV. They are therefore considered relevant in any environment where low-energy electrons are present.

II. Experimental Considerations

A. Principle and Limitations of the Method

Electron capture induced reactions in van der Waals clusters are studied in a beam experiment (Figure 1).
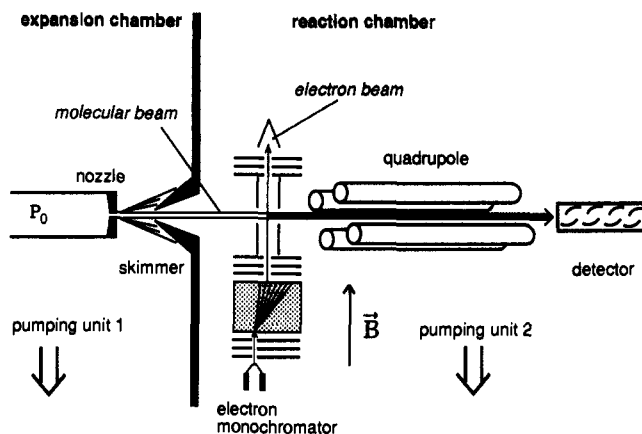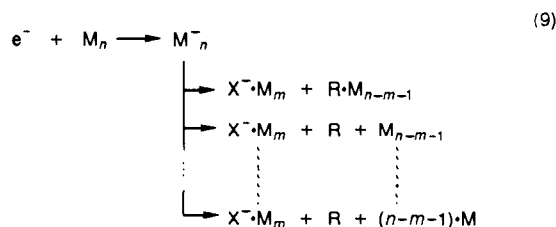

Figure 1. Schematic of the experimental setup for the study of free electron attachment to molecular clusters.

A supersonic beam containing a *distribution* of clusters of different sizes is crossed with a beam of monochromatized electrons. Negative ions resulting from this interaction are detected by a quadrupole mass spectrometer. The excess translational energy of the product ions can be determined by a time-of-flight (TOF) technique through the quadrupole as briefly described below. It should be emphasized that electron attachment to an isolated molecule and the subsequent decomposition into one negatively charged and one neutral fragment, viz.,

$$e^- + M \longrightarrow M^{-(*)}$$
$$\longrightarrow R + X^- \qquad (8)$$
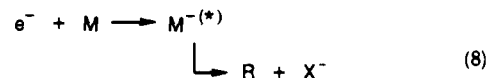
is a convenient way to study the unimolecular decomposition of the ion $M^{-(*)}$. Since the internal energy of the precursor ion is uniquely controlled by the energy of the primary electron, determination of the excess translational energy of the fragment ion (and hence, through momentum conservation, of both fragments, $R + X^-$) yields information on the distribution of the total excess energy (translational and internal) in the unimolecular reaction. In photoionization, such information requires the use of coincidence techniques.

On going to van der Waals aggregates M_n, the situation becomes significantly more complex. A reaction yielding the product $X^- \cdot M_m$, e.g., may proceed along the following scheme:

$$e^- + M_n \longrightarrow M_n^-$$
$$\longrightarrow X^- \cdot M_m + R \cdot M_{n-m-1}$$
$$\longrightarrow X^- \cdot M_m + R + M_{n-m-1}$$
$$\vdots$$
$$\longrightarrow X^- \cdot M_m + R + (n-m-1) \cdot M$$

(9)

From eq 9 it is clear that it is generally not possible to conclude from the observed product $X^- \cdot M_m$ to the size (n) of the target cluster or to the number of neutral products ultimately formed in the decomposition of the ionized target aggregate M_n^-. In electron attachment to the monomer, on the other hand, decomposition into more than one negatively charged and one neutral fragment can usually be excluded from simple energetic reasons. However, since the average size of the cluster
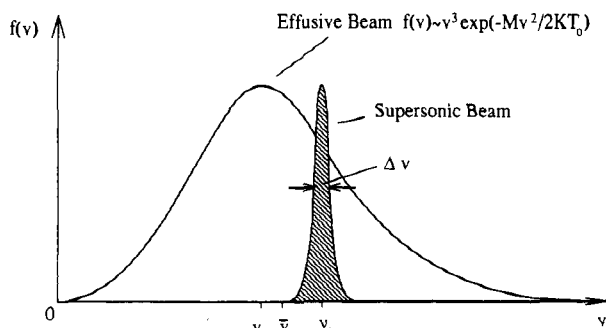
Figure 2. Velocity distribution in an effusive molecular beam and in a supersonic beam.

distribution can be varied to some extent by changing the expansion conditions, one can witness the evolution of the relevant quantities (attachment energies, product ions, and their kinetic energy release) on proceeding from the monomer to clusters of increasing size.

B. Cluster Formation, Electron Beam, and Ion Formation and Detection

In our experiment the supersonic beam containing the clusters is formed by adiabatic expansion of the respective gas through an 80-μm nozzle which can be heated and cooled down to liquid nitrogen temperature. The expansion converts the enthalpy associated with random molecular motion into directed mass flow.[2,91-94] This is illustrated in Figure 2: at low stagnation pressure, when the mean free path of the molecules is larger than the nozzle diameter, $\lambda > d$, the molecular beam effusing from the nozzle possesses a velocity-weighted Maxwell–Boltzmann distribution. When $\lambda \ll d$, we have a free jet expansion associated with a narrow velocity distribution. For a monoatomic gas, the terminal velocity can be expressed as

$$v_t = (5kT_0/M)^{1/2} \qquad (10)$$

where T_0 is the temperature of the *source*. The (translational) temperature of the molecules in the beam is determined by the width of the velocity distribution Δv. Under certain assumptions[92,93] Δv and hence the temperature T in the beam is given by

$$\frac{T_0}{T} = \left(\frac{p_0}{p}\right)\frac{1-\kappa}{\kappa} \qquad (11)$$

where $\kappa = c_p/c_v$ and p_0 and p are the stagnation pressure and the pressure in the beam, respectively. In polyatomic molecules we have $\kappa \approx 1$ and cooling is less effective. In this case one applies the *seeded beam* technique. Here the molecules of interest are diluted in an inert carrier gas (He, Ar) which acts as a refrigerant to cool the molecules until they polymerize. Since the molecules are diluted in small amounts in the carrier gas the velocity of the beam is then still approximately given by eq 10 with M now the mass of the carrier gas. If helium is used this can result in large values for the translational energy of clusters in the laboratory frame of reference. As an example, if CF_3Cl is seeded in He, the pentamer $(CF_3Cl)_5$ will move with a translational energy of more than 8 eV along the direction of the beam! In actual practice there is always some "velocity slip" which will lower the beam velocity to some extent. To avoid discrimination in the detection of product

ions due to large translational energies perpendicular to the axis of the mass spectrometer, we have chosen to place the mass spectrometer *in line* with the molecular beam (Figure 1).

After expansion from the nozzle, the beam passes a skimmer (0.8-mm diameter) which separates the expansion chamber from the main chamber. Approximately 7 cm downstream, the molecular beam is crossed at right angles with an electron beam generated by a trochoidal electron monochromator (TEM). This energy filter uses a combination of a magnetic and an electric field.[95,96] Its operation principle is brefily as follows: The electrons emitted from a heated filament are aligned by the homogeneous magnetic field $\vec{B}$ ($\approx$100 G) which is generated by a pair of Helmholtz coils mounted outside the vacuum system. They enter a deflection region defined by the crossing of the magnetic field with the electric field $\vec{E}$ ($\approx$1 V cm^{-1}). The latter is produced by a potential difference between two parallel plates. It is directed into the plane of paper (shaded area in Figure 1). Under the influence of both fields the electrons describe a trochoidal or cycloidal motion depending on whether or not they possess velocity components perpendicular to the beam axis when entering the deflection region. The trochoidal or cycloidal path implies motion of its guiding center with constant velocity perpendicular to both the magnetic

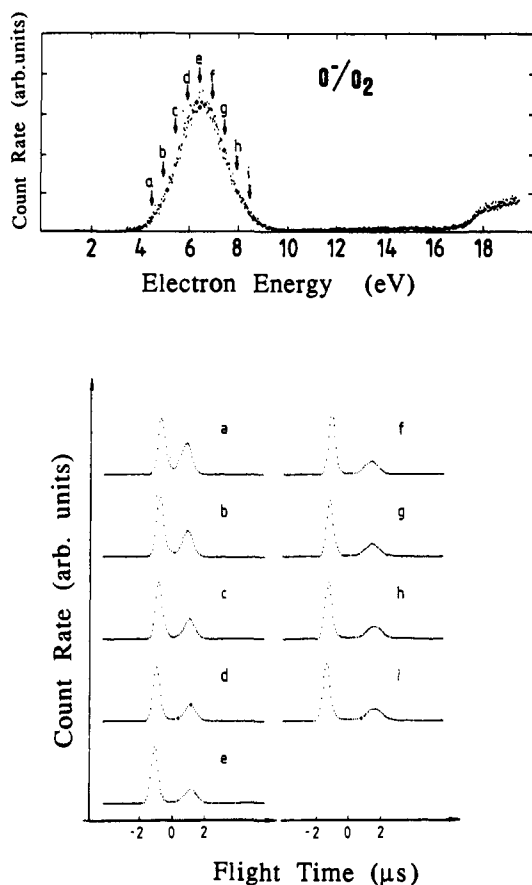$$\vec{v} = \frac{|\vec{E} \times \vec{B}|}{\vec{B}^2} \qquad (12)$$

and the electric field. This results in a dispersion of the electrons according to their axial velocity and only those electrons which reach the exit aperture (displaced by some distance with respect to the entrance aperture) are further transmitted. These energy selected electrons are then accelerated or decelerated by subsequent electrodes before entering the reaction volume.

The combination of a TEM with a quadrupole mass filter has proven to be particularly suited for studying electron attachment reactions since it combines some important necessary properties. (1) The axial magnetic field prevents spreading of the electron beam at low energies so that reasonable intensities (10–100 nA) can be achieved down to very low (thermal) energies. (2) The TEM can be operated in the continuous mode: due to the presence of the magnetic field, the energy of the electrons entering the reaction volume is not disturbed by the (continuous) ion draw out field. This field only causes a slight deflection of the electron beam along a plane of constant electric potential. (3) The alignment of the electron beam by the magnetic field allows the separation of electrons and negative ions at the ion detector (secondary electron multiplier).

For the present experiments, the TEM was operated with an energy resolution of 0.1–0.2 eV (fwhm) and a current of 50–100 nA.

Negative ions arising from the interaction of the electron beam are extracted from the reaction volume, analyzed by a quadrupole mass filter, and detected by single event pulse counting techniques. Ion-yield curves (resonance profiles) are obtained by scanning the electron energy for a given production. This is provided by a multichannel scaling plug in board in an IBM PC.

Figure 3. Schematic of the experimental arrangement for TOF analysis (translational excess energy release) of product ions.

C. Translational Excess Energy of Products

The translational energy analysis of the product ions uses a time of flight (TOF) technique in combination with a quadrupole mass filter as elsewhere described in detail.[2,97,98] In brief, the pulsed electron beam (pulse width < 1 μs) interacts with the molecular beam and the flight time of the ions (generated within the short time of the electron pulse) from the reaction volume through the quadrupole to the detector is measured (Figure 3). The TOF arrangement, in principle, corresponds to a two-field TOF spectrometer, consisting of a draw-out region (ϵ_1 = 4 V cm^{-1}), an acceleration region (ϵ_2 = 30 V cm^{-1}), and the quadrupole mass filter which acts as the drift tube (ϵ = 0). This allows space focusing by adjusting ϵ_1/ϵ_2 to a certain value.[2,98] Since the quadrupole guarantees the mass separation, one can use a low draw-out field (4 V cm^{-1}) in order to visualize excess translational energies on the time scale.

Ions formed with low kinetic energy (e.g., thermal ions) exhibit one peak in the TOF spectrum while ions generated with considerable kinetic energy produce two peaks due to "direct" and "turn around" ions. In the latter case discrimination against velocity components perpendicular to the flight tube axis results in a separation (in time) of ions ejected parallel (direct) or antiparallel (turn around) to the axis. The turn around ions are decelerated, reversed, and then accelerated and reach the detector by some time delay (ΔT) with respect to the direct ions (Figure 3). From the experimentally determined flight time difference (ΔT), the initial kinetic energy release of the product ion can be calculated as

$$E_T^i = \frac{(\Delta T q \epsilon_1)^2}{8 m_i} \qquad (13)$$

where ϵ_1 is the draw-out field introduced above, q the elementary charge, and m_i the mass of the ion.

Conversely, for ions with low kinetic energy (<0.1 eV for the present configuration) there is no discrimination against perpendicular velocity components and all ions are transmitted to the quadrupole. For a Maxwell–Boltzmann velocity distribution, the corresponding TOF peak has a Gaussian shape. Its width $\Delta T_{1/2}$ (fwhm) is related to the average kinetic energy $\bar{E}_T^i$ (= $^3/_2 kT$) by

——— Internuclear Separation ———►

Figure 4. Potential energy curves of O_2 and O_2^- relevant in electron scattering from gaseous O_2.

$$\bar{E}_T^i = \frac{(\Delta T_{1/2} q \epsilon_1)^2}{3.7 m_i} \qquad (14)$$

Recording of the flight times is performed by a time-to-pulse height converter (TPHC) followed by A/D conversion with the plug in board mentioned above, now operating in the pulse height analysis mode (Figure 3).

III. Results and Discussion

A. Oxygen Clusters. Violation of the Selection Rule $\Sigma^+ \leftrightarrow \Sigma^+$ in Electron Attachment. The Role of Inelastic Scattering in the Formation of $(O_2)_n^-$

We shall begin with the diatomic system O_2 where some essential features concerning electron capture by isolated molecules and the corresponding van der Waals clusters can clearly be observed.

Figure 4 shows potential energy curves relevant in resonant electron scattering from gaseous oxygen molecules.[1,2,99–102] It is well established that the adiabatic electron affinity of the oxygen molecule is positive, namely 0.440 eV.[103]

Capture of low-energy electrons, i.e., a Franck–Condon transition from O_2 ($^3\Sigma_g^-$) + e$^-$ to O_2^- ($^2\Pi_g$) forms the anion in its electronic ground state, but vibrationally excited ($v \geq 4$). Due to the absence of operative stabilization mechanisms, O_2^- thus formed has a finite lifetime with respect to autodetachment (10^{-12} to 10^{-10} s[104–106]) far beyond the scale for a mass spectrometric detection. In a high pressure environment, the ion can be stabilized in a three-body process to a vibrational level ($v < 4$) where autodetachment is no longer possible (Bloch–Bradbury mechanism[107]).

A further Franck–Condon transition at higher electron energies generates the anion in a repulsive, electronically excited state, O_2^{*-} ($1\pi_u^{-1}$, $1\pi_g^2$)$^2\Pi_u$. In this case, the incoming electron simultaneously excites an electron in the target molecule resulting in a state with one hole in the $1\pi_u$ MO (assigned as $1\pi_u^{-1}$) and two additional electrons in the $1\pi_g$ MO (assigned as $1\pi_g^2$). We have thus a *two particle–one hole* (2p-1h) resonance as mentioned in the introduction.

Figure 5 shows the experimental result obtained with our "effusive beam apparatus"[2,38] where the electron beam collides with the molecular beam effusing from

Figure 5. Ion-yield curve of O^- from O_2 (top) and TOF spectra of O^- recorded at different electron energies (below).

a capillary under single collision conditions. As in earlier experiments,[101,108] only O^- is observable arising from a broad resonance between 4.5 and 10 eV. The continuous increase of the O^- signal above 17 eV is due to the (nonresonant) ion-pair formation process

$$e^- + O_2 \longrightarrow O_2^{**} + e^-$$
$$ \downarrow$$
$$O^+(^4S) + O^-(^2P) \tag{15}$$
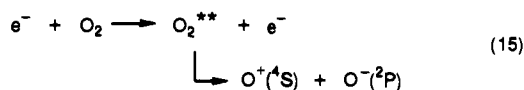
which has an energetic threshold of 17.2 eV.

The shape of the resonance profile of O^- is explained by the *reflection principle*[109] which states that the Franck–Condon factors as a function of energy simply *reflect* the probability density of the ground vibrational state.

Strictly speaking, autodetachment competes with dissociation. Autodetachment is possible until the two dissociating particles reach R_T, the crossing point between the neutral and ionic potential energy curve. For $R > R_T$ the evolution of the system into the two individual fragments, $O + O^-$, has proceeded to such an extent that autodetachment is no longer possible. Dissociative attachment to oxygen shows a strong variation with temperature[110] which was indeed explained by the strong competition between these two channels.[111]

Figure 5 also shows the TOF spectra of O^- recorded at different electron energies. The flight time scale refers to an ion with zero kinetic energy. Direct ions have thus negative and turn around ions positive values. As expected, the separation of the TOF doublet increases with primary electron energy.
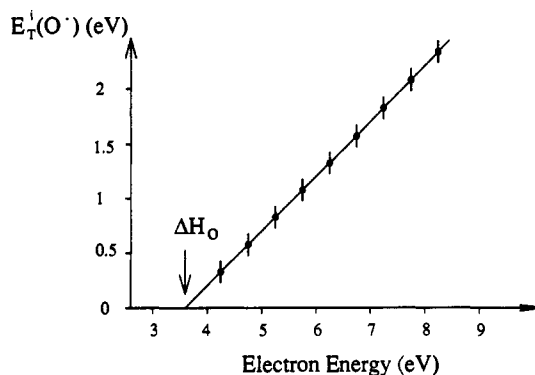
Figure 6. Kinetic excess energy of O^- vs primary electron energy calculated from eq 13.
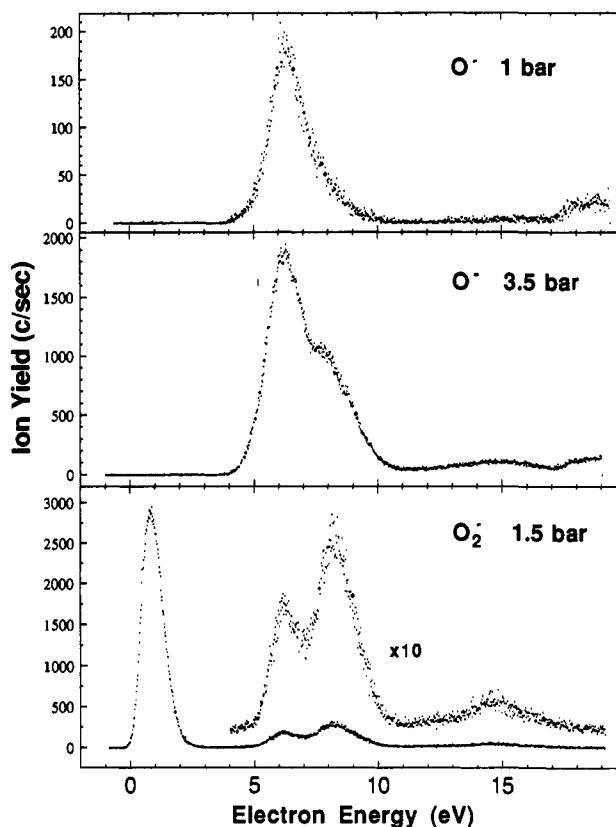
Figure 7. O^- and O_2^- formation following electron attachment in the molecular beam at different stagnation pressures.

In Figure 6 the kinetic energy of O^- calculated according to eq 13 is plotted yielding a straight line with a slope of 0.5 since the translational energy is released in equal amounts to O and O^-. Extrapolation of the line to $E_T^i = 0$ yields the energetic threshold for the reaction, in good agreement with the established thermodynamic value, $\Delta H_0 = 3.60$ eV.

We will now replace single oxygen molecules by oxygen clusters. This is established by expanding pure oxygen through the nozzle which is kept at -80 °C.

In agreement with previous experiments on O_2 clusters by Märk, Stamatovic, and co-workers[48] we observe the two homologous series $(O_2)_n^-$ and $(O_2)_n \cdot O^-$. Figure 7 presents the ion yield curves of O^- and O_2^- at different stagnation pressures. The shape of the O^- signal recorded at 1 bar is similar to that under effusive conditions (Figure 5). On proceeding to a higher stagnation pressure (3.5 bar) we observe the evolution of two distinct new features at ≈ 8.3 eV and ≈ 14.5 eV.

Interestingly, the new feature is even more pronounced in the O_2^- profile at a comparatively low stagnation pressure (1.5 bar). Formation of $(O_2)_n^-$ at very low energies has clearly been demonstrated in the previous work of Märk et al.;[48] it is an illustrative example of the "built in" many body stabilization mechanism in a cluster. As will be shown below, formation of ions of the form $(O_2)_n^-$ and $(O_2)_n \cdot O^-$ at energies above 4 eV is likely to originate from completely different mechanisms.

For the explanation of the additional features at 8.3 eV and 14.5 eV in the channels $(O_2)_n \cdot O^-$ we refer to recent experiments on electron stimulated desorption (ESD) of O^- from O_2 multilayer films performed by Sanche et al.[112-115] (see also section IV) and to a study of dissociative electron attachment to singlet oxygen, O_2 ($^1\Delta_g$).[116,117] Analysis of the O^- ion yield between 4 and 15 eV in the electron stimulated desorption study can be explained by considering the negative ion states O_2^- lying below 15 eV.[118,119] Although a variety of O_2^- states can be formed from O and O^- [24 states, e.g., from ground state $O(^3P)$ and $O^-(^2P)$!] only few of these possess the proper characteristics for dissociative electron attachment. Molecular orbital analysis[120] of the states joining the two lowest limits indicates that only the $^2\Pi_u$, $^2\Sigma_g^+$, and $^2\Sigma_u^+$ states are relevant for dissociative attachment. (They must be repulsive in the Franck–Condon region, and spin conservation requires a doublet or quartet state.)

Out of these states the Σ^+ configurations cannot be formed in elect attachment to isolated O_2 from the $^3\Sigma_g^-$ ground state. Since in the single-electron–molecule frame of reference a one-electron wave function must principally be σ^+, transitions from Σ^- to Σ^+ and vice versa are forbidden (σ^--selection rule).[37] This selection rule holds in electron attachment and autoionization. The electron stimulated desorption experiments, along with the theoretical analysis, lead to the conclusion that the excited negative ion states, $^2\Sigma_g^+$ and $^2\Sigma_u^+$, are responsible for the O^- yield observed near 8 and 14 eV, respectively. This was considered the first experimental evidence for the violation of the σ^--selection rule in electron attachment.

In light of these findings we conclude that the structures appearing near 8.3 and 14 eV in the channels $(O_2)_n \cdot O^-$ are also due to electron attachment via the symmetry forbidden states O_2^{*-} ($3\sigma_g^{-1}$ $1\pi_g^2$) $^2\Sigma_g^+$ and O_2^{*-} ($2\sigma_u^{-1}$ $1\pi_g^2$)$^2\Sigma_u^+$. The existence of an additional state between 8 and 9 eV is further supported by our recent dissociative attachment study to O_2 ($^1\Delta_g$)[116] (Figure 8). In this experiment, part of the oxygen molecules were excited into the long-lived singlet state (excitation energy 0.98 eV) in a microwave discharge. The three contributions in Figure 8 were ascribed to dissociative electron attachment from (1) ground-state O_2 ($^3\Sigma_g^-$) and (2) singlet O_2 ($^1\Delta_g$) oxygen via the O_2^{*-} ($^2\Pi_u$) negative ion state and (3) from O_2 ($^1\Delta_g$) via the O_2^{*-} ($^2\Sigma_g^+$) state. The latter contribution peaks at 7.5 eV corresponding to an energy of 8.5 eV with respect to ground state O_2 ($^3\Sigma_g^-$).

Figure 9 shows a schematic of the associated potential energy curves. From analysis of the kinetic energy release,[116,117] it is established that the O_2^{*-} ($^2\Sigma_g^+$) state predominantly decomposes into the second dissociation limit, $O^-(^2P) + O(^1D)$. We thus conclude that all odd
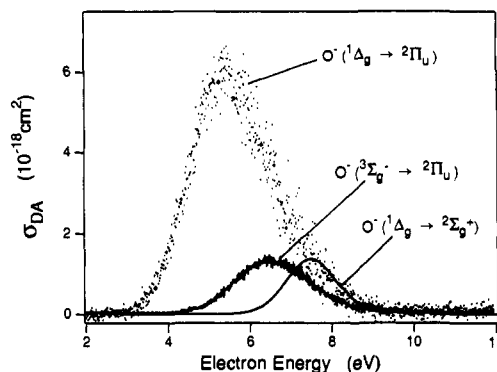

Figure 8. Cross section for dissociative electron attachment to ground-state O_2 ($^3\Sigma_g^-$) and singlet-state O_2 ($^1\Delta_g$) oxygen molecules.
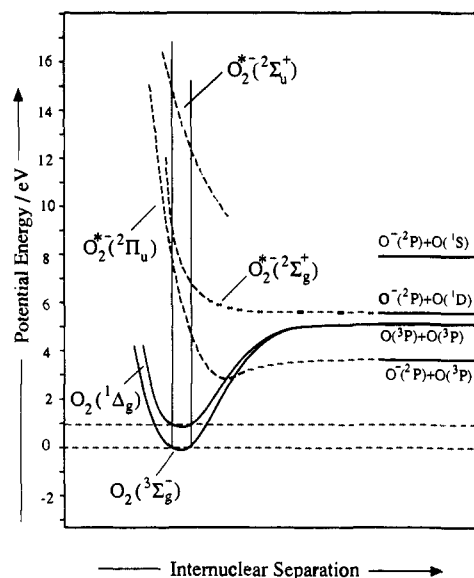

Internuclear Separation ⟶

Figure 9. Potential energy diagram of O_2 and O_2^-. Only those negative-ion states are shown which are considered relevant in dissociative electron attachment (see text).

number cluster anions $(O_2)_n \cdot O^-$ have O^- as precursor which is formed via dissociative electron attachment to the repulsive Π_u, Σ_g^+, and Σ_u^+ states.

The question now arises on the mechanism of $(O_2)_n^-$ formation at energies above 4 eV. While it is clear that at low energies these anions are formed through the electronic ground state O_2^- ($^2\Pi_g$) and subsequent collisional stabilization, it is rather unlikely to establish a reasonable mechanism to explain formation of $(O_2)_n^-$ through the initial population of the strongly repulsive Π_u, Σ_g^+, and Σ_u^+ states. In large clusters, on the other hand, cage effects may indeed prevent the dissociation of the pair $O^- + O$ ultimately leading to $(O_2)_n^-$. The experimental observation is that the relative intensities in the $(O_2)_n^-$ yield are virtually independent of stagnation pressure[121] (i.e. the average cluster size in the beam) while this is not the case for $(O_2)_n \cdot O^-$. As an example Figure 10 shows the $(O_2) \cdot O^-$ yield at increasing stagnation pressure indicating the enhanced contribution of the symmetry forbidden transitions as the average size of the cluster increases.

In light of this we interpret $(O_2)_n^-$ formation at electron energies above 4 eV as a result of a *secondary reaction*: the incoming electron is inelastically scattered (through direct and resonant scattering, the latter involving the O_2^{*-} resonances) in the cluster and the
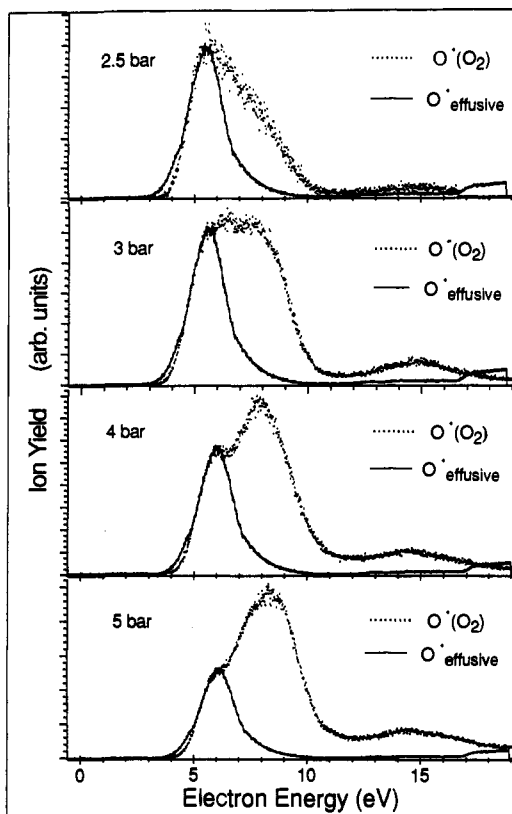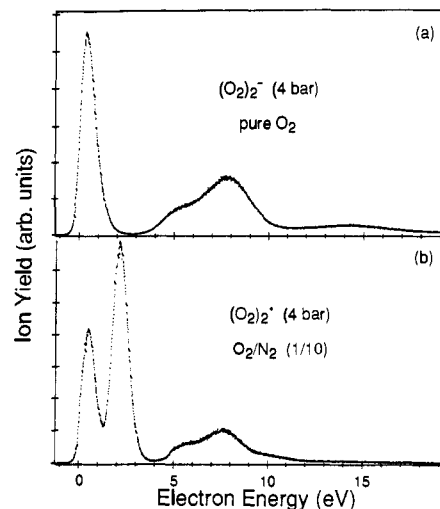
Figure 10. Yield of $O_2 \cdot O^-$ for different stagnation pressures showing the enhanced contribution of the symmetry forbidden transitions as the cluster size increases.
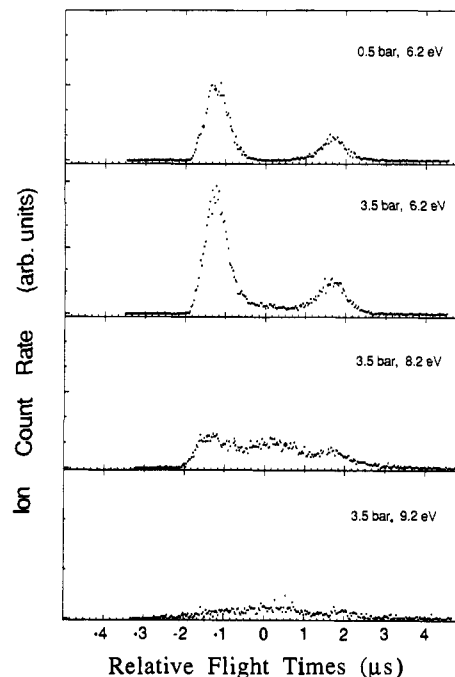

Figure 11. O_4^- formation from mixed N_2/O_2 clusters: (a) $(O_2)_2^-$ from pure oxygen; (b) $(O_2)_2^-$ from N_2/O_2 clusters (10:1). The strong contribution at 2.3 eV is due to inelastic scattering of the primary electron via the N_2^- ($^2\Pi_g$) resonance.

Figure 12. TOF distribution of O^- at different stagnation pressures and electron energies.

slowed down electron is captured forming $(O_2)_n^-$. This picture is supported by the threshold excitation spectrum of oxygen which exhibits pronounced maxima at 6 and 8.3 eV.[122] A threshold excitation spectrum is obtained when the primary energy is scanned and only those electrons are recorded which have lost their total energy. Recent studies on mixed clusters by Märk et al.[123,124] and our own laboratory[121,125] have further shown the role of inelastic scattering for anion formation in mixed clusters. It appears that these secondary processes contribute considerably to anion formation when one component of the system possesses a low-energy resonance which is generally associated with a high capture cross section. As an example, Figure 11 shows the result when a mixture of oxygen and nitrogen (mixing ratio 1:10) is expanded. The dominant feature in the O_4^- channel is now a contribution near 2.3 eV which arises from *resonant inelastic* scattering via the N_2^- ($^2\Pi_g$) negative ion state. This clearly demonstrates the strong contribution of inelastic scattering (in the present case through a resonance of a nonattaching molecule) to negative ion formation in clusters.

We were not able[126] to detect any signal corresponding to m/e = 48, 80, 112, ..., near 0 eV electron energy as previously reported.[127] This signal was interpreted to arise from the formation of doubly charged ions $(O_2)_n^{2-}$, n = 3, 5, 7, ..., in electron attachment to oxygen clusters.

We have also performed TOF experiments in order to get information on the excess kinetic energy release of the product ions. Figure 12 shows some results for the channel O^-. At low stagnation pressure and ϵ = 6.2 eV we observe essentially the feature known from the isolated molecule. At 3.5 bar there is some contribution of signal between the TOF doublet caused by ions

ejected with comparatively low kinetic energy. Although we do not know the exact ratio between monomers and clusters in the beam at 3.5 bar, the intensity ratio $O^-:O_2^-:O_3^-$ = 1:0.6:2 (at 6.2 eV) and the fact that the intensity of O_2^- and O_4^- from the low-energy peak is more than 1 magnitude larger than O^- at 6.2 eV indicate that at –80 °C and 3.5 bar we have considerably more clusters in the beam than monomers.

Figure 13 additionally shows the negative-ion mass spectrum recorded from the low-energy peak at 3.5 bar. Although from the above discussion it is clear that such a mass spectrum (even when recorded near 0 eV and regardless of experimental effects such as discrimination against large masses in a quadrupole) is the result of fragmentation processes following electron capture, it clearly indicates that there are clusters of considerable size in the beam at that stagnation pressure.
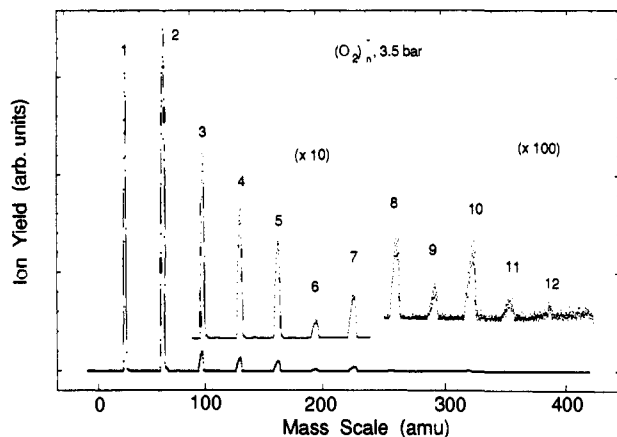
Figure 13. Negative-ion mass spectra recorded from the low-energy resonance.

Figure 14. Negative-ion mass spectrum observed in electron attachment to CF_3Cl clusters.

In any case, the TOF distribution of O^- recorded at 6.2 eV is quite surprising since it indicates that O^- ejection from clusters is essentially the same as for monomers. This is a definitely different behavior from what we know from clusters composed of larger molecules, see below. On going to higher electron energies (population of the $^2\Sigma_g^+$ state), a broad and unstructured TOF distribution appears which remains the only feature at 9.2 eV. This broad TOF distribution reflects a structureless kinetic energy distribution ranging from 0 eV to $\approx$1.5 eV.

An explanation for this behavior is that the O_2^{*-} ($^2\Pi_u$) state is predominantly formed at the "surface" of the target cluster where O^- is emitted with an energy comparable to that in the isolated O_2 molecule.

Conversely, the O_2^{*-} ($^2\Sigma_g^+$) state is created without positional preference in the target cluster and emission of O^- is generally associated with a multiple scattering process within the cluster, resulting in the broad distribution of kinetic energy.

The formation of $(O_2)_n^-$, on the other hand, is always associated with low kinetic energy from any of the resonances and independent of stagnation pressure[128] (not shown here). This supports the *secondary* mechanism involving attachment by an inelastically scattered slow electron.

Photodetachment studies on the system $(O_2)_n^-$ performed by Johnson et al.[129] showed a large jump in electron binding energy from 0.44 eV for the monomer to 1 eV for the dimer with a more gradual, monotonic increase for larger n. In connection with recent thermochemical work on $(O_2)_n^-$ [130] it was concluded that a cluster ion $(O_2)_n^-$ consists of an O_4^- core surrounded by loosely bound O_2 ligands.

In conclusion, it can be seen that negative ion formation in oxygen clusters proceeds via different processes (i) dissociative electron attachment involving the three repulsive states $^2\Pi_u$, $^2\Sigma_g^+$, and $^2\Sigma_u^+$, generating ions of the form $(O_2)_n \cdot O^-$. In single molecules, population of the Σ^+ states is symmetry forbidden, (ii) formation of $(O_2)_n^-$ at low energies (<2 eV) by associative attachment with subsequent collisional stabilization thereby evaporating the target cluster ("evaporative electron attachment"[45]), and (iii) inelastic electron scattering followed by associative attachment of the slowed down electron.
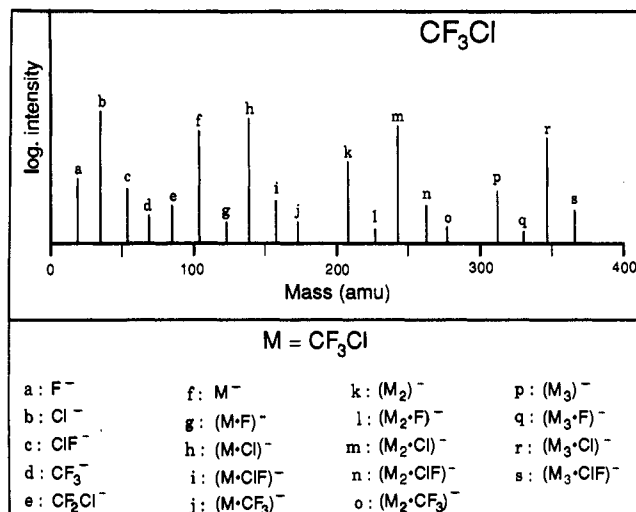
B. Homogeneous Clusters of Polyatomic Molecules

This section presents some recent results obtained in homogeneous clusters composed from molecules which are also well characterized with respect to electron capture by the isolated compounds in the gas phase.

1. Trifluorochloromethane. Distribution of Excess Energy in the Decomposition of Clusters

CF_3Cl possesses two resonances centered around 1.4 eV and 4–5 eV.[38,131] While the low-energy state exclusively yields Cl^-, the electronic state near 4–5 eV decomposes into a variety of negatively charged fragments such as Cl^-, F^-, CF_3^-, etc. The low-energy state is interpreted as one particle resonance, with the additional electron in the first virtual MO which has a strongly localized $\sigma^*(C-Cl)$ antibonding character. TOF experiments, in fact, revealed that the temporary negative ion decomposes *directly* into Cl^- + CF_3 via electronic dissociation along a repulsive potential energy surface.[97]

On proceeding to clusters, we observe a variety of additional, negatively charged complexes. Figure 14 shows the lower part of the negative-ion mass spectrum obtained in electron impact to a cluster beam of CF_3Cl. The beam was generated by adiabatic expansion of CF_3Cl seeded in Ar (1:10) at 2-bar stagnation pressure. The diagram is a superposition of two spectra recorded at electron energies of 1.4 and 4.5 eV, respectively. For a clearer representation, Figure 14 only shows peaks corresponding to ^{35}Cl. Apart from the fragments known from the isolated molecule, one detects a variety of larger charged complexes with the series M_n^-, $M_n \cdot Cl^-$, $M_n \cdot F^-$, $M_n \cdot CF^-$, and $M_n \cdot CF_3^-$.[65,66] As pointed out above, the product ion intensity distribution does not directly reflect the size distribution of the neutral clusters in the beam.

How do the resonance profiles of these product ions behave? Figure 15 shows a few representative ion-yield curves taken at 2-bar stagnation pressure. These spectra have been recorded with a nonmonochromatized electron beam (hairpin filament followed by a series of electrodes instead of the electron monochromator, Figure 1). In spite of the low-energy resolution for the
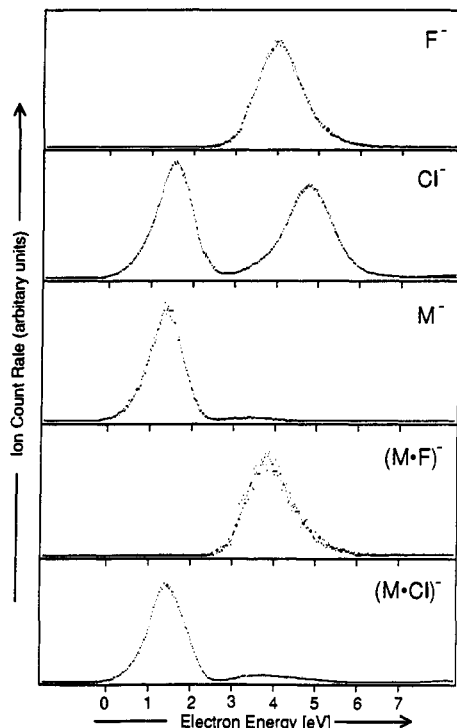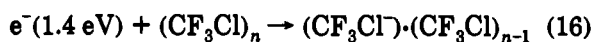
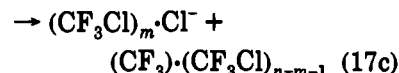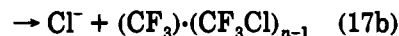**Figure 15.** Some selected ion-yield curves observed in electron attachment to CF_3Cl clusters.

present experiment ($\Delta\epsilon \approx 0.7$ eV, fwhm), we see that all the ions are formed within a low-energy resonance and/or a resonance between 4 and 5 eV already known from the isolated compound. The shapes and energetic positions of these ion-yield curves do not depend on the stagnation pressure, at least not to an extent observable at the poor resolution. The only significant effect is the observation that the relative intensity of the low-energy Cl^- signal with respect to the one at 4.8 eV increases with stagnation pressure (see below).

The ions M_n^- and $M_n \cdot Cl^-$ are predominantly formed from the resonance of low energy, and $M_n \cdot F^-$ is solely associated with the second resonance and closely resembles the F^- ion yield. The shapes of the ion-yield curves are virtually independent of n. All products appear within a resonance near 1.4 eV and/or a resonance of higher energy (4–5 eV) already known in the isolated molecule. This indicates that electron capture by CF_3Cl clusters proceeds via initial formation of an individual anion (CF_3Cl^-) in the aggregate whose initial state is not much affected by the surrounding constituents of the target cluster. While the isolated molecule decomposes into the different fragments, the ionized cluster gives rise to the many different product ions apparent in the mass spectrum (Figure 14). There is no indication of anion formation via inelastic scattering prior to electron capture.

We will now restrict the discussion to low-energy attachment associated with the electronic ground state of CF_3Cl^-. In the isolated molecule this resonance decomposes by direct electronic dissociation exclusively into $Cl^- + CF_3$. In the aggregate, we have formation of a localized anion in a repulsive state:

$$e^-(1.4\text{ eV}) + (CF_3Cl)_n \rightarrow (CF_3Cl^-)\cdot(CF_3Cl)_{n-1} \quad (16)$$

which evolves according to

$$(CF_3Cl^-)(CF_3Cl)_{n-1} \rightarrow (CF_3Cl)_m^- + (CF_3Cl)_{n-m} \quad (17a)$$

$$\rightarrow Cl^- + (CF_3)\cdot(CF_3Cl)_{n-1} \quad (17b)$$

$$\rightarrow (CF_3Cl)_m\cdot Cl^- + (CF_3)\cdot(CF_3Cl)_{n-m-1} \quad (17c)$$

In eqs 17a–c each neutral channel is assigned to consist of only one compound. Of course, as in the case of oxygen clusters, the reactions will generally release enough excess energy for a further evaporation of the target cluster. Channel 17a, $m = 1$, leaves the parent radical anion in its relaxed configuration. This implies that the potential energy surface of M^- in its electronic ground state must possess a minimum as illustrated in Figure 16. For the present system, a relaxation energy of more than 1.4 eV (at resonance maximum) has to be distributed in the target cluster.

Figure 17 demonstrates how the TOF distribution evolves with increasing stagnation pressure and hence the average size of clusters in the beam.

At low stagnation pressure (0.5 bar, Figure 17a) one observes a separated TOF doublet similar to that for the isolated system.[97] At that pressure there is no indication of cluster formation and Cl^- arises solely from electron capture by monomers. The quantitative evaluation of the TOF spectrum shows that virtually all of the available excess energy is transferred into kinetic energy of $Cl^- + CF_3$. The decomposition of the isolated ion is an example of the "rigid radical" limit within the impulsive model for dissociation.[132,133] In the present example, CF_3 behaves like a rigid radical, and the decomposition of the polyatomic molecule is analogous to that of a diatomic molecule. It should be noted that polyatomic negative ions generally do not behave according to the impulsive model. They rather decompose by a more or less effective distribution of the available excess energy among the different degrees of freedom.[134,135]
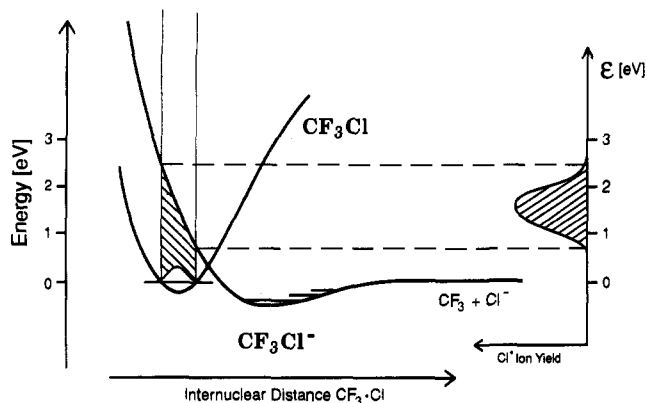
By increasing the stagnation pressure (1 bar) an additional feature near time zero becomes apparent. This contribution dominates the spectrum at 3 bar. Any further increase in pressure leaves the TOF distribution virtually unchanged.

Figure 17d shows the result of a graphical subtraction which indicates that the TOF spectrum consists of two components, one due to Cl^- ions with considerable kinetic energy and an additional one yielding low-energy ions.

So far, we have demonstrated that cluster formation coincides with the appearance of low-energy Cl^- ions. The question concerning the origin of the high-energy component (which is still present in the TOF spectra at high stagnation pressures), however, is still open. This feature may be due to Cl^- emission from monomers (in the beam or from background gas) or from particular clusters.

If target clusters exist with structures where the F_3C-Cl axis points away from the other molecules one would expect the free emission of Cl^- ions and, thus, a behavior similar to the isolated case.

On the other hand, for configurations in which the $F_3C–Cl$ axis of the temporary ion points toward other members of the target cluster one expects either the

**Figure 16.** Potential energy diagram illustrating dissociative electron attachment to CF_3Cl (see text).
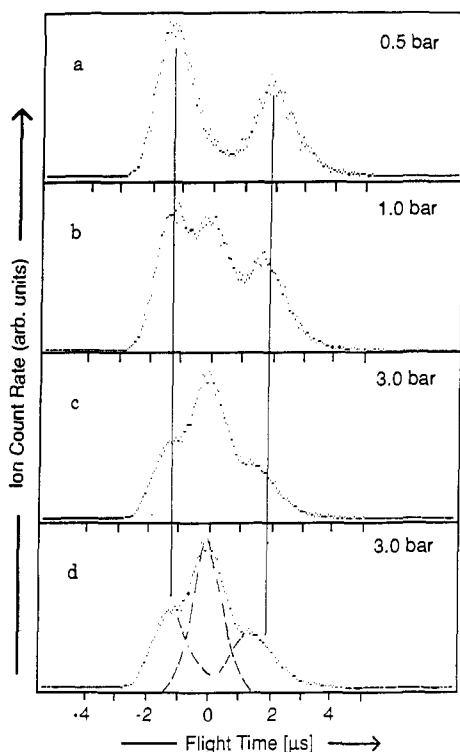
Figure 17. Evolution of the Cl^-/CF_3Cl TOF spectrum with increasing stagnation pressure recorded at the resonance maximum (1.4 eV).

emission of low-energy Cl^- ions, slowed down by scattering events or the ultimate formation of the other products observed at that energy (CF_3Cl^-, M_n^-, or $M_n \cdot Cl^-$).

TOF experiments with helium as carrier gas have shown[136] that the high-energy component is, in fact, predominantly due to Cl^- emission from scattered background monomers and only a small amount is due to Cl^- emission from targets in the supersonic beam: If helium is used as carrier gas, the velocity of the particles in the beam (i.e. along the axis of the flight tube) is very high and in a TOF spectrum one can easily distinguish between Cl^- emission from particles traveling with the seeded beam velocity and Cl^- emission from background molecules. The present system thus behaves in a different way compared with oxygen discussed above: the amount of translational energy arising from dissociation of a repulsive electronic state is drastically reduced in CF_3Cl on proceeding to clusters. In oxygen, on the other hand, ejection of O^- from the
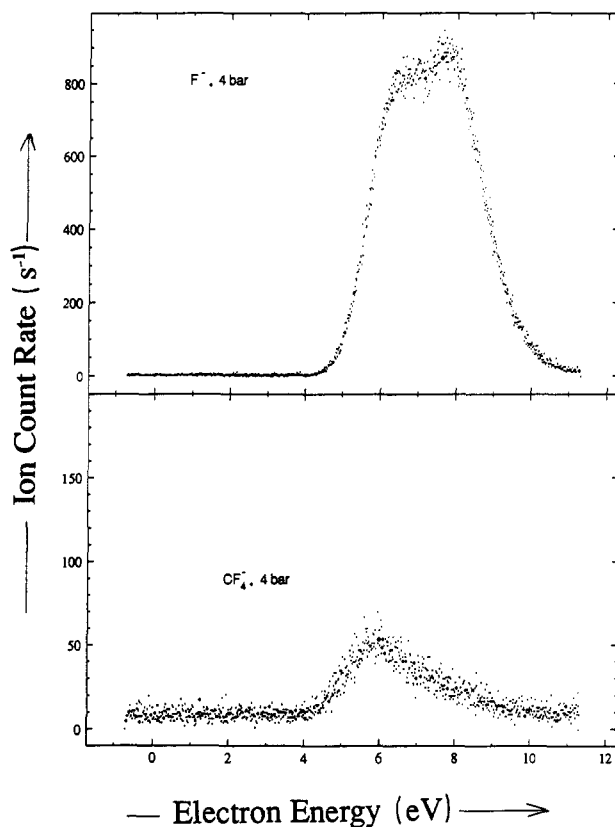
— Electron Energy (eV) ⟶

Figure 18. Formation of F^- and CF_4^- following electron attachment to CF_4 clusters.

$O_2^{*-}(^2\Pi_u)$ state remains virtually unchanged between monomers and clusters.

The appearance of low-energy Cl^- ions from CF_3Cl clusters is also responsible for the enhanced Cl^- intensity from the low-energy resonance mentioned above. The explanation is that thermal ions are much less discriminated by the ion draw out configuration than energetic ions.[98]

The present example demonstrates that intermolecular energy transfer in the aggregate allows the preparation of molecular anions not accessible by other techniques. To our knowledge, CF_3Cl^- has not been observed in the gas phase before. The effect of intermolecular energy transfer becomes much more dramatic in the case of CF_4 clusters.

2. Tetrafluoromethane. Observation of CF_4^-

CF_4 captures electrons within a broad resonance centered around 7-8 eV which is associated with the formation of F^- and CF_3^-.[38,98]

On proceeding to clusters, we find a variety of additional products i.e. F_2^- and the series M_n^-, $M_n \cdot F^-$, and $M_n \cdot CF_3^-$. Among these, the appearance of CF_4^- is most surprising. This ion has not been observed before.

The ion-yield curves show that all products are formed within the broad resonance region known from electron capture by the monomer.[67] Their individual shape, however, varies significantly from one product to another. All members of the series $M_n \cdot CF_3^-$ virtually coincide with the CF_3^- profile while the maximum of the formation probability of CF_4^- (and the other members of the series M_n^-) is shifted to significantly lower energies.[67] As an example, Figure 18 shows the ion yield curves for CF_4^- compared with F^-. These

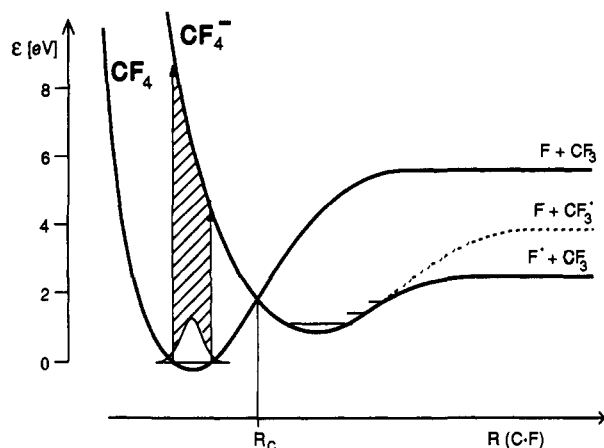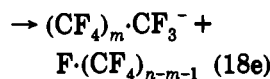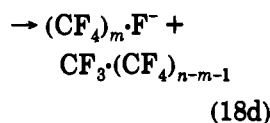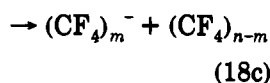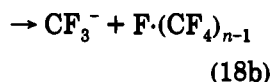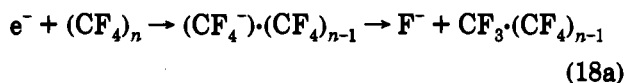**Figure 19.** Hypothetical potential energy diagram for CF_4 and CF_4^- (see text).

spectra are recorded with a monochromatized electron beam at a stagnation pressure of 4 bar.

From experiments on isolated CF_4 we know that the temporary ion CF_4^- is formed in a strongly repulsive state which immediately decomposes into the channels $F^- + CF_3$ and $CF_3^- + F$ with considerable release of kinetic energy to the fragments. If CF_4^- is formed within an aggregate, we must consider the following reactions:

$$e^- + (CF_4)_n \rightarrow (CF_4^-) \cdot (CF_4)_{n-1} \rightarrow F^- + CF_3 \cdot (CF_4)_{n-1}$$

$$(18a)$$

$$\rightarrow CF_3^- + F \cdot (CF_4)_{n-1}$$

$$(18b)$$

$$\rightarrow (CF_4)_m^- + (CF_4)_{n-m}$$

$$(18c)$$

$$\rightarrow (CF_4)_m \cdot F^- + CF_3 \cdot (CF_4)_{n-m-1}$$

$$(18d)$$

$$\rightarrow (CF_4)_m \cdot CF_3^- + F \cdot (CF_4)_{n-m-1} \quad (18e)$$

Observation of CF_4^- again implies that its potential energy surface must possess a minimum at an energy *below* the lowest dissociation channel, i.e., $F^- + CF_3$, which lies 2.26 ± 0.13 eV above the neutral ground state of CF_4 [taking established values for the F_3C-F bond dissociation energy $(5.66 \pm 0.13$ eV[137] and the electron affinity of F $(3.399 \pm 0.003$ eV[138])].

A hypothetical potential energy diagram for CF_4 and CF_4^- in their respective electronic ground states is shown in Figure 19. If CF_4^- is ultimately formed in its equilibrium configuration, a relaxation energy of up to 6 eV has to be distributed among the target aggregate! This can only occur by a substantial evaporation of the initial cluster. It is not yet established whether or not CF_4 possesses a *positive adiabatic electron affinity*. Figure 19 illustrates the ion in a *metastable* state. Although the energy of the relaxed ion is above that of ground-state CF_4 (negative adiabatic electron affinity), the Franck-Condon overlap to the ground state is

extremely poor, preventing the ion from autodetachment. The diagram further suggests that CF_4^- represents a weakly bound adduct $CF_3 \cdot F^-$ (with one bond significantly weakened) rather than a tetrahedral CF_4^-. We have here a similar situation to the system CO_2 mentioned in the introduction: although it is well known that the monomer has a negative EA, electron attachment to clusters also yields the metastable monomer anion CO_2^-,[47,56,157] which, due to its bent structure, has a poor Franck-Condon overlap to the linear ground state.

Returning to the ion-yield curve (Figure 18), the most significant feature here is the asymmetric profile of the M^--yield curve toward lower energies within the resonance.

The cross section for the formation of a specific ion X^- can be written as

$$\sigma(X^-) = \sigma_0 \cdot P(X^-)$$

with σ_0 the attachment cross section of the target compound and $P(X^-)$ the probability for the formation of X^- with respect to other competitive channels, including autodetachment. If $P(X^-)$ does not depend on energy, we can write $\sigma(X^-) \sim \sigma_0$ and the line shape of the ion-yield curve will have a Gaussian profile based on the reflection principle. For more complex reactions $P(X^-)$ generally depends on the energy of the precursor ion which will influence the peak shape of the ion-yield curve. It is plausible that CF_4^- formed at the lower energy side of the resonance has a higher chance of being stabilized, since less relaxation energy has to be distributed among the target aggregate. This results in an ion-yield curve with an asymmetric profile.

As in the case of CF_3Cl, a TOF analysis performed on CF_4 shows that the ejection of F^- and CF_3^- is effectively slowed down when proceeding to clusters.[67]

3. Acetonitrile. Formation of Dipole-Bound CH_3CN^-

The interaction of an electron with a stationary dipole has been of considerable interest over the past decade since it provides the possibility of negative molecular ions not accessible with conventional MO type interaction. It has been predicted[139,140] that all molecules with dipole moments greater than ≈ 2 D are able to form a dipole supported state, i.e., an electronic state in which an extra electron is weakly bound in the field of the dipole. For molecules possessing a positive electron affinity, a dipole-supported state represents an electronically excited state of the anion. Such states have been observed in photodetachment spectroscopy from enolate and o-benzoquinone anions.[141-143] Here, transitions from ground state create dipole-supported states of finite lifetime (dependent on the rotational energy) with respect to detachment of the additional electron.

For acetonitrile, on the other hand, electron-scattering experiments and MNDO calculations predict a negative electron affinity $(-2.84$ eV).[144,145] Its dipole moment is 3.92 D and thus well beyond the critical value. The experimental evidence for the existence of a dipole supported state, however, was rather conflicting. The thermal electron attachment rate was found to be unmeasurably low while in collisions with highly excited Rydberg rare gas atoms CH_3CN^- was observed.[146-148] In contrast to that, collisional electron
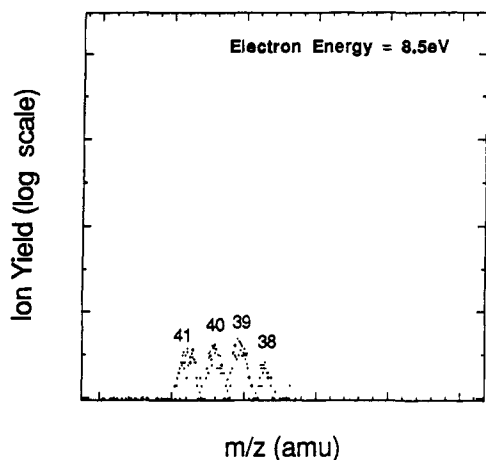
Figure 20. Negative ion mass spectrum from clusters of CH_3CN recorded at 8.5 eV electron energy and at a stagnation pressure of 1 bar.

transfer to a distribution of CH_3CN clusters (including monomers) from Rydberg krypton atoms yielded $(CH_3CN)_n^-$, $n \geq 13$ but no CH_3CN^-.[84] Attempts to detect CH_3CN^- in collisions with fast alkali atoms also failed.[149]

In previous experiments on isolated CH_3CN it was shown that dissociative electron attachment is characterized by an unusually low cross section.[145] Two resonances were observed with peak maxima at 3 eV and near 8 eV. They decompose into various fragments (CH_3^-, CN^-, C_2N^-, C_2HN^-, and $C_2H_2N^-$) with $C_2H_2N^-$ the dominant ion. The low-energy resonance was interpreted as a shape resonance due to involvement of the π_{CN}^* MO and the second one as core excited resonance with two electrons in normally unfilled MOs. We here discuss the formation of dipole-bound CH_3CN^- through electron attachment to CH_3CN clusters.

Acetonitrile clusters were prepared by flowing Ar through a stainless steel vessel containing liquid acetonitrile and expanding the mixture through the nozzle. From clusters we additionally observe ions of the form $CH_2CN^-\cdot(CH_3CN)_n$.[70] They are predominantly formed at a stagnation pressure near 1 bar and arise within the two resonances known from the isolated molecule. In addition, there is strong evidence that acetonitrile anion, CH_3CN^- is exclusively formed within the *second* resonance.

Figure 20 shows the relevant section of the mass spectrum obtained at 8.5-eV electron impact to the CH_3CN cluster beam at a stagnation pressure of 1 bar. We assign the observed mass numbers to C_2N^- (38), C_2HN^- (39), CH_2CN^- (40), and CH_3CN^- (41).

Upon decreasing the stagnation pressure, both the CH_3CN^- signal and the signal due to $CH_2CN^-\cdot(CH_3CN)_n$ decrease until they disappear. The mass spectrum then corresponds to that recorded under effusive gas inlet which was provided by a capillary directly connected to the reaction chamber. The mass spectrum then still contains a small signal at $M = 41$. Since its intensity is $\approx 2\%$ of $M = 40$ we assign it to $^{13}CH_2CN^-$.

Figure 21 presents ion-yield curves of the mass numbers 40 and 41 recorded at 1-bar stagnation pressure. Cyanomethyl anion (CH_2CN^-) is, like in the effusive case, predominantly formed within the low-energy resonance. As can be seen from the absolute count rate in Figure 21, the $M = 41$ signal at 3 eV is
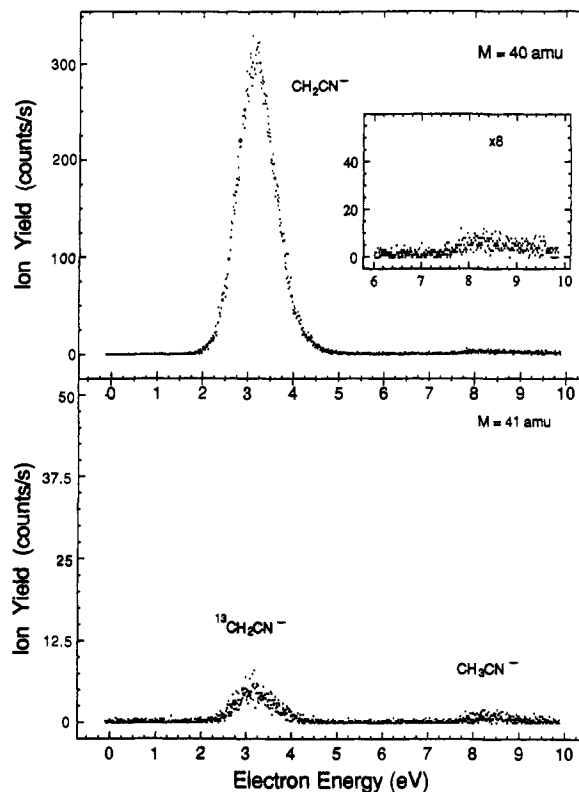
Figure 21. Ion-yield curves of $M = 40$ amu and $M = 41$ amu recorded at 1-bar stagnation pressure. Note the different scale for the ion-count rate.
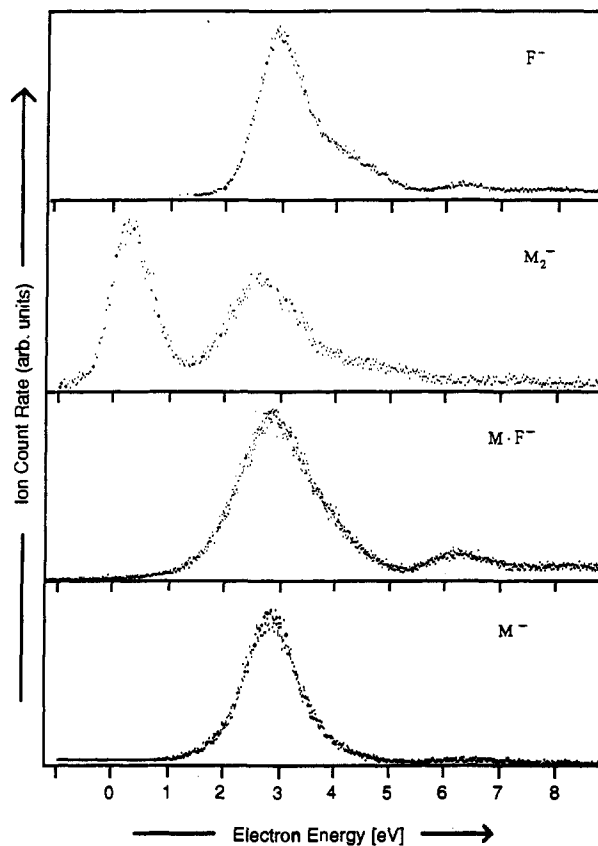
Figure 22. Some selected ion-yield curves obtained in electron attachment to C_2F_4 clusters.

$\approx 2\%$ of $M = 40$ and must thus be due to cyanomethyl anion with one ^{13}C atom. On the other hand, the $M = 41$ signal near 8.5 eV is of comparable intensity,

consistent with the mass spectrum (Figure 20), and we assign it to CH_3CN^-. Although very weak in intensity its resonance profile is obvious. This indicates that CH_3CN^- formation is in fact a result of electron attachment to CH_3CN clusters and not due to collisional charge transfer with excited species which may also be present at that energy.

It is quite remarkable that only electron capture near 8.5 eV provides the conditions to generate an observable acetonitrile anion. Obviously, the core excited state provides the access to form the dipole bound state rather than electron-transfer or low-energy electron attachment to CH_3CN.

It should, however, be noted that one cannot a priori rule out the formation of isomers of acetonitrile such as the radical anion of aminoacetylene, azirine, or vinylnitrene.

Some of the corresponding neutrals are experimentally known; their energy is predicted to lie considerably above acetonitrile, e.g., 100 kcal in the case of vinylnitrene.[150] To our knowledge, however, the existence of the anions is not known. From all the experimental results presented here it is also clear that electron attachment to clusters forms (among other channels) the anion in its energetically lowest configuration. In the case of $C_2H_3N^-$ this is dipole bound CH_3CN^-.

4. Tetrafluoroethylene. Appearance of a Low Lying Electronic State in $(C_2F_4)_n^-$, $n \geq 2$

It is well known that electron capture in C_2F_4 gives rise to an isolated resonance peaking at 3 eV.[151] This electronic state is described by accommodation of the excess electron into the lowest virtual orbital having π^* character. The $C_2F_4^-$ $(^2\Pi)$ resonance then decomposes into channels yielding F^-, CF_3^-, CF_2^-, and CF_3^-.[152,153]

In clusters we observe the expected resonance near 3 eV yielding all the fragments known from the monomer and, additionally, various larger complexes such as M_n^-, $M_n \cdot F^-$, etc. The ion-yield curves for the larger products are shifted by 0.2–0.5 eV toward lower energies.

The most striking feature is the appearance of an additional resonance at low energy. This electronic state is coupled exclusively with the formation of M_n^- $(n \geq 2)$! It should be noted that negatively charged monomers are readily observed (Figure 22) from the 3-eV resonance. It is yet not clear whether the monomeric anion represents a thermodynamic stable ion or a metastable compound comparable to CF_4^- discussed above. Ab initio calculations predict an EA near 0 eV.[154] Figure 22 gives a few ion-yield curves recorded at a stagnation pressure of 2 bar. F^- formation is not expected from the low-energy resonance for simple energetic reasons, since the C–F bond energy exceeds the electron affinity of F by approximately 1.5 eV. It is, however, surprising that the radical anion M^- is not formed at low energy although it is clearly seen from the higher energy resonance (Figure 22).

It is also striking that, among all larger compounds, M_2^- is formed with an extraordinarily high intensity and one might think that the sample contains some impurity of perfluorocyclobutane which, in fact, captures low-energy electrons to form a long-lived radical anion like other cyclic perfluoro compounds.[155] However, experiments at low stagnation pressure did not

show any indication of an M_2^- signal, and we conclude that this ion must be a product of electron capture by clusters of perfluoroethylene.

What is the nature of this new electronic state? It is likely that M_2^- in its *relaxed* form represents a stable cyclobutane anion, but this says nothing about the initial state of the excess electron in the target aggregate at the instant of the electronic transition. In the present system, the response of the charge distribution toward the incoming electron obviously changes when proceeding from monomer to aggregate.

As mentioned in the Introduction, the formation of a temporary negative ion in an atom or molecule is usually described by the long-range interaction between the electron and the neutral particle. This interaction and thus the vertical attachment energy is largely determined by the polarizability of the neutral compound. If the aggregate or a particular structure in it possesses a larger polarizability than the isolated compound, there will always be the possibility of trapping an excess electron at a lower energy. In a somewhat simplified view, one would expect for clusters in which the intermolecular distances are large compared with the bond length in a molecule that the incident electron would interact primarily with one individual molecule. The localized anion M^- is formed in an electronic state not significantly perturbed by the other molecules.

Conversely, if particular clusters or structures within them exist that allow a more collective response of the charge distribution with respect to the incoming electron, one would expect electron capture to occur at a lower energy.

The low-energy absorption band shows an intriguing pressure dependence when monitoring the M_2^- ion-yield curve.[69,156] By increasing the stagnation pressure, one first observes the low-energy absorption band, and only at higher stagnation pressures does the $^2\Pi$ resonance (shifted to lower energies by 0.5 eV) become apparent. The same behavior can be noted for all members of the series M_n^- $(n \geq 2)$, with the general trend that the signal onset arises at higher stagnation pressures with increasing n. This suggests that small clusters (probably dimers due to their significantly high intensity) represent the specific structure that allows low-energy electron absorption.

Although the occurrence of an additional low-energy resonance in clusters was observed in various other systems,[56,157] it is not clear whether this is a general feature in aggregates consisting of larger polyatomics. Clusters of perfluoroethane[156] or methanol,[126] for example, only absorb electrons near the energy known from the isolated molecule. Studies in trifluoroethylene,[157] on the other hand, also reveal an additional low-energy peak associated with M_n^- $(n \geq 2)$.

C. Heterogeneous Clusters

We shall finally present some results from heterogeneous clusters which are composed of molecules possessing resonances at considerably different energies. The obvious question then arises as to whether product ions composed of *both* constituents are formed. In section III.A we have already presented a result in mixed N_2/O_2 clusters. In this case, N_2 as a nonattaching
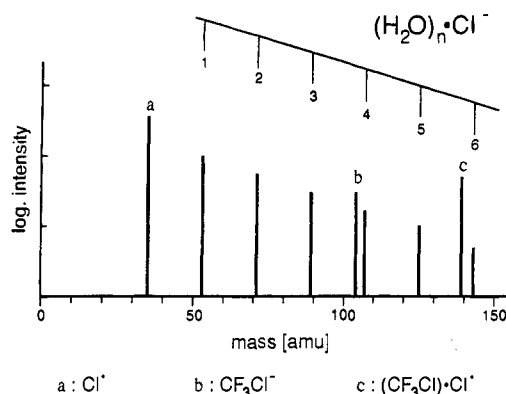
Figure 23. Negative-ion mass spectrum recorded at 1.4 eV electron energy from heterogeneous clusters composed of H_2O and CF_3Cl.

component considerably contributes to $(O_2)_n^-$ formation through inelastic scattering of the primary electrons.

1. CF_3Cl/H_2O. Formation of Solvated Ions

As discussed above, trifluorochloromethane exhibits two clearly separated resonances near 1.4 eV and 4–5 eV, while H_2O captures electrons within three overlapping resonances between 6.5 and 12 eV which are associated with the formation of H^-, O^-, and OH^-.[158,159] For the channel $H^- + OH$, it has been established that most of the excess energy is released as kinetic energy to the fragments.[160]

The heterogeneous clusters are prepared by flowing CF_3Cl seeded in Ar (1:10) at a pressure of 1.8 bar through a stainless steel vessel containing liquid water near room temperature and expanding the mixture through the nozzle as described in Experimental Considerations.

Although the clusters under consideration are composed of simple molecules, the assignment of the mass spectrum is not in any case straightforward. In the 0–10 eV region the negative-ion mass spectrum shows evidence for the solvated ions $[(H_2O)_n \cdot Cl^-$ $(n \geq 1)$, $(H_2O)_n \cdot F^-$ $(n \geq 1)$, and $(H_2O)_n \cdot OH^-$ $(n \geq 2)]$ and all the products obtained in electron capture by homogeneous CF_3Cl aggregates described above, as well as O^- and OH^-. We have restricted our experiments to mass numbers below 150 so that the possible formation of $(H_2O)_n^-$ $(n \geq 11)$[32] has not been a subject of the present investigations. The assignment of the mass spectrum is sometimes ambiguous since different possible compounds have identical mass numbers. For example, $CF_3Cl \cdot Cl^-$ (mass numbers 139, 141, and 143) overlaps with $(H_2O)_6 \cdot Cl^-$ (143/145), $(H_2O)_7 \cdot OH^-$ (143), and $(H_2O)_7 \cdot F^-$ (145). They can, however, sometimes be distinguished by their different energy dependences.

Figure 23 shows the lower part of a mass spectrum recorded at 1.4 eV electron energy. Only peaks due to ^{35}Cl are shown. We ascribe the mass numbers 53, 71, 89, 107, 125, and 143 to $(H_2O)_n \cdot ^{35}Cl^-$ $(n = 1–6$, see below).

In Figure 24 we have recorded the ion yields corresponding to mass numbers 35, 53, 55, and 19 in the energy range 0–12 eV. Above 11 eV, one observes a continuously rising signal which cannot be discriminated by mass filter or any electrostatic potential. This signal is easily identified as arising from electronically excited carrier gas atoms in their well-known metastable states, Ar^* $(^3P_2, 11.55\,eV)$, Ar^* $(^3P_0, 11.72\,eV)$,[161] causing electron emission at the first dynode of the electron multiplier.
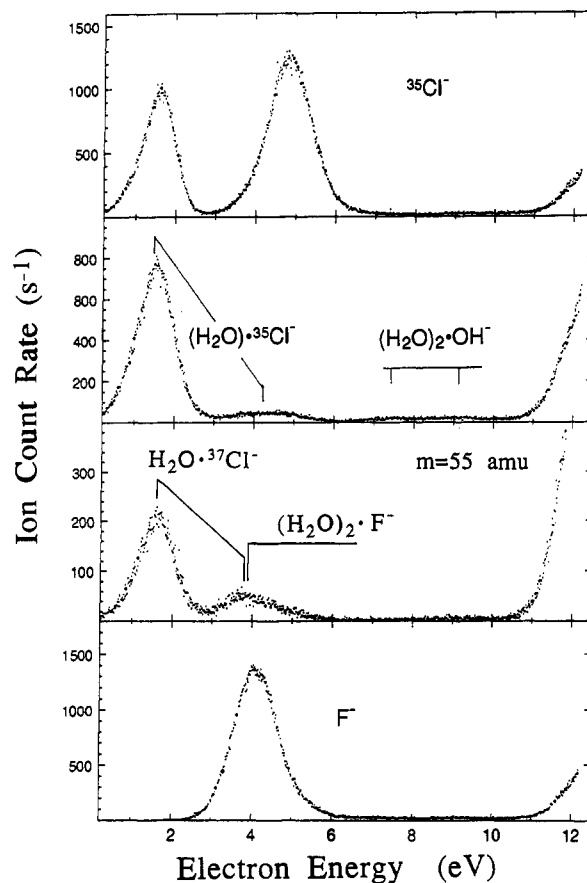
Figure 24. Selected ion-yield curves obtained in electron attachment to clusters composed of H_2O and CF_3Cl (see text).

Figure 24a gives the $^{35}Cl^-$ yield which is similar to that obtained from homogeneous CF_3Cl clusters (Figure 15). In the ion-yield curve recorded for $M = 53$ (Figure 24b) we assign the signals near 1.4 and 4.5 eV to $H_2O \cdot ^{35}Cl^-$ and the weak contribution above 7 eV to $(H_2O)_2 \cdot OH^-$. Solvated hydroxyl ions $(H_2O)_n \cdot OH^-$ $(n \geq 2)$ have also been detected between 7 and 10 eV in electron impact to H_2O clusters.[32] As expected, the ion yield recorded at $M = 55$ (Figure 24c) gives no contribution near 7 eV; the intensity ratio between the two low-energy resonances, however, differs substantially from that in Figure 24b. We interpret the signal near 4–5 eV as being composed of $(H_2O) \cdot ^{37}Cl^-$ and $(H_2O)_2 \cdot F^-$. Solvated ions of the type $(H_2O)_n \cdot F^-$ $(n \geq 1)$ can, in fact, be observed in clusters composed of H_2O and perfluorinated compounds arising at energies close to that of F^- formation. For comparison, Figure 24d shows the F^- yield.

The present example illustrates that the formation of the solvated ions $(H_2O)_n \cdot Cl^-$ proceeds predominantly through the low-energy resonance of CF_3Cl at 1.4 eV. From the results presented above, we know that this molecular anion is generated in a strongly repulsive $C–Cl^-$ electronic state.

2. CF_2Cl_2/O_2. Chemical Reactions Induced by Slow Electrons

Single difluorodichloromethane captures electrons at low energies (<1 eV) and also within a resonance near 3–4 eV.[2,38,131] Low-energy electron attachment is exclusively associated with dissociative attachment into $Cl^- + CF_2Cl$ which is by far the dominant reaction. On
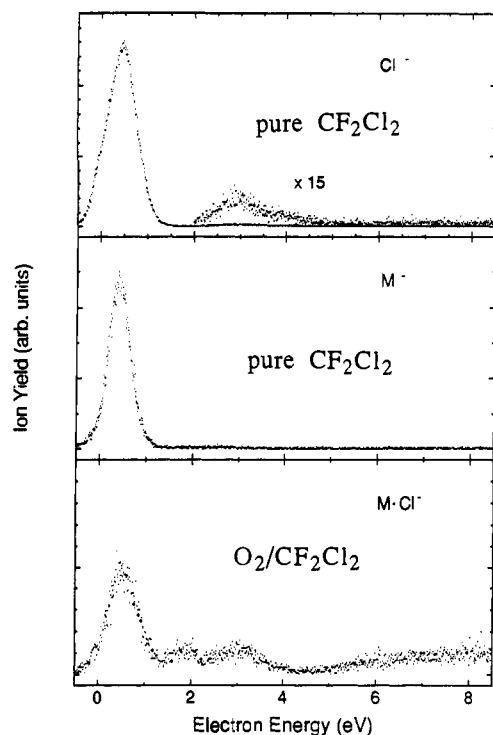
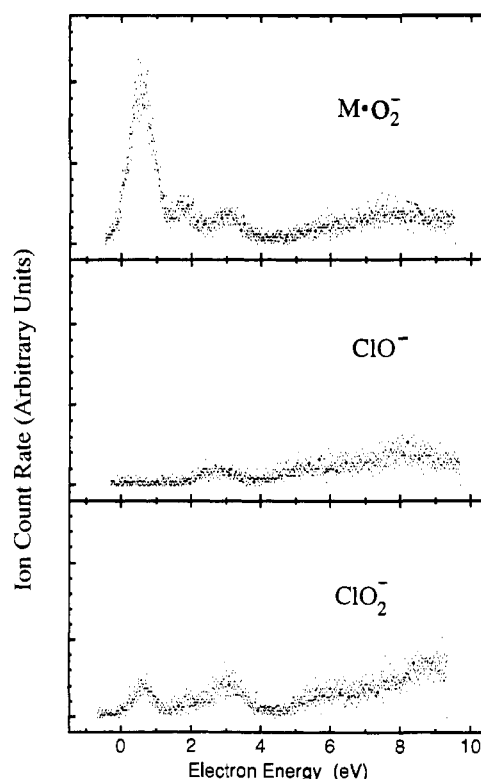**Figure 25.** Energy profiles of ion formation in pure and mixed clusters, M=CF_2Cl_2: (a) Cl^- formation; (b) M^- formation from pure CF_2Cl_2 clusters; (c) $M \cdot Cl^-$ formation from clusters containing O_2 and CF_2Cl_2 (see text).

Figure 26. Energy profiles of ion formation from clusters containing O_2 and CF_2Cl_2.

proceeding to CF_2Cl_2 clusters, one observes a variety of negatively charged product ions, among them the homologous series M_n^-, $M_n \cdot Cl^-$, and $M_n \cdot F^-$. Figure 25a,b shows the channels Cl^- and M^- observed from *pure* CF_2Cl_2 clusters. When a *mixture* of CF_2Cl_2 and O_2 is expanded, we observe product ions composed of *both* cluster constituents. In addition, for most of the product ions formed, there is now a significant contribution to the ion signal for primary electron energies above 5 eV. In Figures 25c and 26a–c the energy dependences of some product ions are plotted. These spectra were recorded with a mixture of CF_2Cl_2:$O_2 \approx$ 1:100 at 2-bar stagnation pressure and a nozzle temperature of $-40\,°C$. Both $M \cdot Cl^-$ and $M \cdot O_2^-$ show marked resonances near 0.7, 1.8, and ≈ 3 eV and some broad and overlapping structure near 6 and 8 eV. Processes induced near 0.7 eV may either proceed via initial electron attachment to an O_2 or CF_2Cl_2 molecule within the target clusters. However, at 3 eV it is likely that the primary step is formation of a $CF_2Cl_2^-$ ion and, accordingly, at 6 and 8 eV the formation of O_2^{*-} ($^2\Pi_u$) and O_2^{*-} ($^2\Sigma_g^+$), respectively. Generation of $M \cdot Cl^-$ at 6 and 8 eV is thus expected to proceed via electron capture by O_2 and subsequent electron transfer ultimately releasing $M \cdot Cl^-$.

The product ClO^-, on the other hand, is formed considerably above 1 eV. Although weak in intensity, a resonancelike profile near 3, 6, and 8 eV is obvious. It is the result of a complex reaction associated with the cleavage of *two* chemical bonds and the formation of a *new* molecule. The weak intensity does not allow one to measure a reliable pressure dependence of its signal, so we cannot definitely conclude that ClO^- is the result of a reaction within *one isolated* cluster. The energy profile, however, suggests that the reaction can either be induced through electron capture by O_2 or by CF_2Cl_2.

The ClO_x compounds play a particular role in the chemistry of the Earth's atmosphere,[162,163] and their thermochemistry is well characterized.[164] The energetic threshold of ClO^- formation from isolated O_2 and CF_2Cl_2 can be estimated as ΔH_0 = 3.4 eV, taking $D(CF_2Cl-Cl)$ = 3.3 eV, $D(O-O)$ = 5.12 eV, $D(Cl-O)$ = 2.75 eV[165] and $EA(ClO)$ = 2.25 eV.[166] In clusters this value may be lowered to some degree due to possible reaction pathways with energetically favorable neutral products. The experimentally observed threshold is near 2 eV (Figure 26b).

The product ions arising from mixed clusters also exhibit a significant structure at 1.8 eV which does neither appear from pure oxygen clusters nor from CF_2Cl_2 clusters. This peak may be a result of a particular, *inelastic* scattering process in the target cluster followed by low-energy electron capture; it may also be due to an *electronic state* which is established by the *collective response* of O_2 and CF_2Cl_2 toward the incoming electron.

IV. Relation to the Condensed Phase

As mentioned in the Introduction, clusters represent a *link* between matter in its gaseous and condensed form.

Electron scattering experiments from "condensed" matter have been performed in many different ways, from molecules adsorbed in submonolayer on certain surfaces to multilayer molecular (more or less ordered) films.

One may divide such studies into two main categories, namely those where the energy loss of the backscattered electrons (and eventually the angular dependence) is recorded[167–169] or others where the reaction products of the scattering process are identified.[169–170] The last category includes desorption induced by electronic
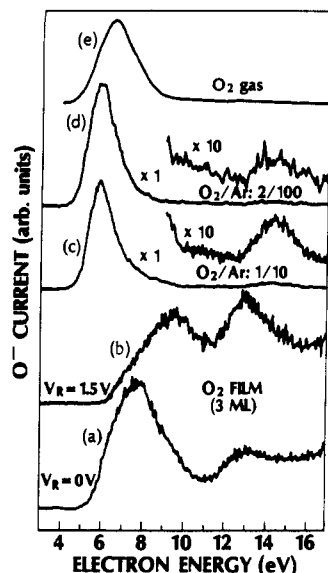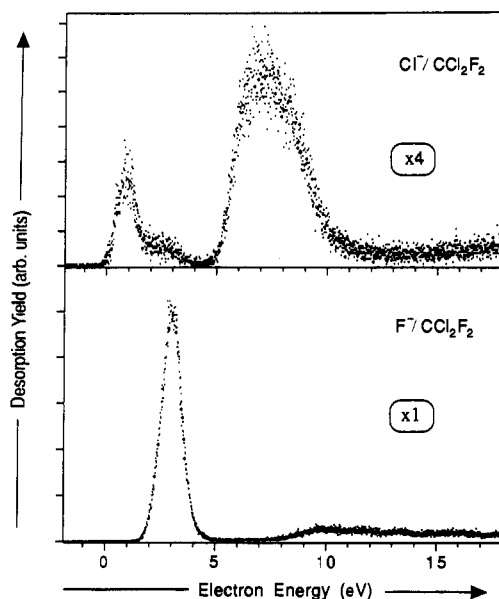
Figure 27. Electron stimulated O^- desorption yield from O_2 and Ar/O_2 films: (a,b) 3 monolayers O_2; V_R is a potential retarding the desorbing ions before entering the mass filter; (c,d) 20 monolayer Ar film containing 10% and 2% volume O_2, respectively; (e) gas-phase O^- yield (from ref 114).

transitions (DIET) which has increasingly been studied within the last decade.[171-174] In the case of *electron* impact induced reactions, the vast majority of experiments were performed in the energy range above 20 eV. The study of processes at energies below 20 eV is virtually restricted to the work of Sanche et al. (for reviews, see refs 114, 115, and 176). It was shown that elastic scattering can only be explained in terms of solid-state concepts while inelastic interactions are interpreted by invoking resonant scattering at a molecular site.

In the discussion of oxygen clusters we have referred to the work of electron scattering from multilayer oxygen films, where resonances—similar to those in clusters—could be observed by measuring the desorbed negatively charged O^- fragment. Further studies involving desorption of negative ions have been carried out for condensed molecules of NO and N_2O,[176] Cl_2,[177] CO,[112] H_2O,[178] and a series of hydrocarbons.[179]

Figure 27 shows the ion-yield curves of O^- from condensed oxygen performed by Sanche et al.[114] The desorption yield is measured for a three monolayer O_2 film (a and b) and a 20 monolayer Ar film containing 10% (c) and 2% volume O_2 (d). For comparison, O^- formation from gaseous O_2 is plotted in Figure 27e (see also Figure 5). The molecules are condensed on a clean, electrically isolated polycrystalline platinum (Pt) ribbon press fitted on the cold tip of a closed-cycle refrigerated cryostat. All components (sample, electron gun, and mass spectrometer) are housed in an ultrahigh vacuum (UHV) chamber reaching pressures below 5×10^{-11} mbar.

Curve b in Figure 27 was recorded by retarding the ions with a potential of -1.5 eV prior to entering the mass spectrometer. As the concentration of O_2 molecules increases (the molecules are then less isolated from each other), additional features near 8 and 14 eV appear which are ascribed to the symmetry forbidden transitions discussed in section II.A.


Figure 28. Electron-stimulated desorption of fragment ions from a multilayer of condensed CF_2Cl_2 (see text).

This was the first experimental evidence for the violation of the σ^- selection rule. The result also demonstrates that electron scattering from condensed molecules is reasonably described in terms of potential energy diagrams at a molecular site.

Figure 28 shows a recent result of electron-stimulated desorption from condensed CF_2Cl_2 observed in our laboratory,[180] and for comparison, negative-ion formation from the isolated molecule (Figure 29). The gas-phase spectrum shows a resonance at 0.8 eV and near 3–4 eV; the resonance at low energy is exclusively coupled with Cl^- formation. No significant ion signal is observed above 5 eV in the gas phase. Similarly, electron capture by clusters of CF_2Cl_2 yields ions also near 0.8 and 3–4 eV (see Figure 25a). Electron-stimulated desorption from condensed CF_2Cl_2, on the other hand, gives an *additional* "resonance like" contribution shifted by 6–6.5 eV with respect to the gas-phase resonance. In the Cl^- yield the width and energetic position closely resembles the first absorption band of neutral CF_2Cl_2.[181-183] We therefore suggest that the first electronically excited state is involved in the quasi-resonant contribution at higher energies. This can proceed either by inelastic scattering of the incoming electron at a molecule on or near the surface. The scattered slow electron is then resonantly captured by a second molecule which decomposes, giving the desorbed fragment ions. Another possibility is inelastic scattering followed by a further interaction of the slow electron with the excited molecule. In contrast to the gas phase, the scattered electron can be backscattered and subjected to an additional interaction with the excited molecule during its short lifetime. As mentioned above, such interactions can have enormous cross sections. However, to elucidate the reaction mechanism of this second contribution, more sophisticated experiments have to be carried out. From the scale factors in Figures 28 and 29 it can be seen, that in the gas-phase formation of Cl^- is the dominant channel while it is F^- in the condensed phase.

The present examples demonstrate that low-energy electrons can also be reactive when they interact with
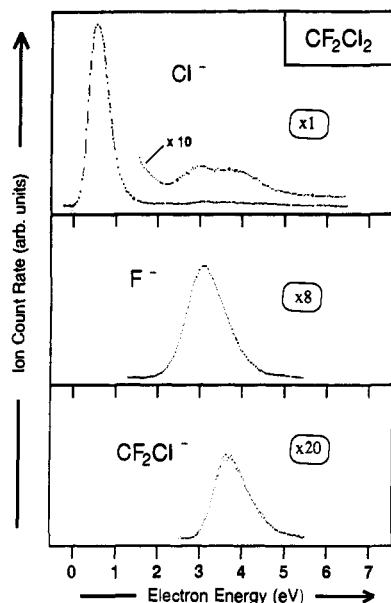
Figure 29. Negative-ion formation from isolated CF_2Cl_2 under single collision conditions.

condensed matter: injection of low-energy electrons into a multilayer film results in the ejection of fragment ions into vacuum.

V. Conclusions and Further Prospects

From the results presented here, it can be seen that the study of electron-attachment reactions to molecular aggregates allows new insight into fundamental problems concerning low-energy interactions with matter. With respect to the *primary* step of electron attachment we have shown that (1) the cluster environment can facilitate the population of negative ion states which are not accessible in the single electron–molecule frame of reference and (2) the collective response of the molecules representing the cluster can provide the condition to trap the excess charge at energies for which the isolated molecule is transparent. If the excess charge is localized by forming an individual temporary anion in the cluster, the *evolution* of the molecular ion proceeds via multiple scattering events involving inter- and intramolecular charge and energy transfer. Among these are many-body stabilization processes leaving the molecular anion in its energetically lowest state. In heterogeneous clusters, more complex processes result in the formation of solvated ions or new ions composed from both cluster components. It was further shown that in clusters composed of molecules having the ability to capture electrons near 0 eV, inelastic scattering processes prior to attachment can significantly contribute to negative-ion formation.

These studies suffer from two essential shortcomings: (a) lack of direct information on the *exact size* of the cluster from which the product is observed and (b) lack of *structural information* on the target aggregate.

The first shortcoming can principally be overcome by subjecting the neutral cluster beam to a scattering process with a rare gas beam as introduced by Buck et al.[184,185] Due to momentum transfer in the scattering process, the clusters in the beam are dispersed according to their size, i.e. light clusters are scattered into large scattering angles and vice versa. This technique has

been used for infrared predissociation experiments on size-selected van der Waals clusters[186–188] [$(C_2H_4)_n$, $(C_6H_6)_n$, $(SF_6)_n$, $n = 2$–6, and the hydrogen-bonded systems $(NH_3)_n$ and $(CH_3OH)_n$]. The obtained spectra contain valuable structural information on the corresponding clusters.

To our knowledge, for the systems treated in this article, no structural information is available from spectroscopic data.

Although sophisticated ab initio calculations allow reliable information on small *elemental* clusters (Na_n, K_n, Li_n, etc., including their cations and anions; for a review, see Bonačić-Koutecký et al.[189]), and probably small clusters composed from diatomic or triatomic molecules, these methods are no longer adequate to treat larger van der Waals clusters of organic molecules. A reasonable method to theoretically investigate such systems may emerge from the use of intermolecular pair potentials which were determined for some halogenated methanes from ab initio and experimental data.[190]

The results presented here were obtained on clusters composed from molecules in their *electronic ground states*. To date, only a few experiments on electron scattering from excited targets have been performed. Electron capture by singlet oxygen (Figure 8) is one of the rare examples. On the other hand, in many processes, e.g., in discharges or, generally, when electromagnetic radiation interacts with matter, (slow) electrons *and* excited molecules may concomitantly be present. From the rare experimental material it is known that the electron-attachment cross section is strongly enhanced, when the target is in an excited state. In singlet oxygen (Figure 8, excitation energy 0.98 eV) the enhancement factor is about 5. Electron-swarm experiments[191–193] indicate enhancements of more than 6 orders of magnitude, when larger molecules are excited into the first (or higher) electronic states! The relevance of such processes in any environment is obvious where slow electrons and excited molecules are present.

It seems therefore a challenging issue to study such reactions in *beam experiments*, where the energetics and reaction pathways can explicitly be followed.

References

(1) Christophorou, L. G., Ed. *Electron-Molecule Interactions and Their Applications*; Academic Press: Orlando, 1984; Vols. I and II.

(2) Illenberger, E. In *Gaseous Ions, Topics in Physical Chemistry*; Baumgärtel, H., Franck, E. U., Grünbein, W., Eds.; Steinkopff Verlag: Darmstadt: New York, 1992; Vol. II.

(3) Jortner, J., Pullman, A., Pullman, B., Eds. *Large Finite Systems*; Reidel: Dordrecht, 1987.

(4) Benedek, G., Martin, T. P., Pacchioni, G., Eds. *Elemental and Molecular Clusters*; Springer: Berlin, 1988.

(5) Maier, J. P., Ed. *Ion and Cluster Ion Spectroscopy and Structure*; Elsevier: Amsterdam, 1989.

(6) *Z. Phys. D* **19 20**, 1991 (Special Issue, *Proceedings ISSPIC 5, 5th International Symposium on Small Particles and Inorganic Clusters*, Konstanz 1990).

(7) *Int. J. Mass Spectrom. Ion Processes* **1990**, *102*. The entire issue (1) is devoted to ionic clusters.

(8) Ng, C. Y., Ed. *Vacuum Ultraviolet Photoionization and Photodissociation of Molecules and Clusters*; World Scientific Publishing Co.: Singapore, 1991.

(9) Bernstein, E. R., Ed. *Cluster Spectroscopy*; Elsevier: Amsterdam, 1988.

(10) Pikaev, A. K. *The Solvated Electron in Radiation Chemistry*; Israel Program of Scientific Translations: Jerusalem, 1971.

(11) Drzaic, P. S.; Marks, J.; Brauman, J. I. In *Gas Phase Ion Chemistry*; Bowers, M. T., Ed.; Academic Press: Orlando, 1984; Vol. III.

(12) Wetzel, D. M.; Brauman, J. I. *Chem. Rev.* **1987**, *87*, 607.

(13) Lacmann, K. In *Potential Energy Surfaces*; Lawley, K. P., Ed.; Wiley: New York, 1980.

(14) Kebarle, P.; Chowdhurry, S. *Chem. Rev.* **1987**, *87*, 513.

(15) Sanche, L.; Schulz, G. J. *Phys. Rev. A* **1972**, *5*, 1672.

(16) Sanche, L.; Schulz, G. J. *Phys. Rev. A* **1972**, *6*, 69.

(17) Schulz, G. J. *Rev. Mod. Phys.* **1973**, *45*, 378.

(18) Schulz, G. J. *Rev. Mod. Phys.* **1973**, *45*, 423.

(19) Jordan, K. D.; Burrow, P. D. *Chem. Rev.* **1987**, *87*, 557.

(20) Hasted, J. B.; Mathur, D. In *Electron-Molecule Interactions and Their Applications*; Christophorou, L. G., Ed.; Academic Press: Orlando, 1987; Vol. I.

(21) Allan, D. *J. Electron Spectrosc. Relat. Phenom.* **1989**, *48*, 219.

(22) Eland, J. H. D. *Photoelectron Spectroscopy*; Butterworths: London, 1984.

(23) Rabalais, J. W. *Principles of Ultraviolet Photoelectron Spectroscopy*; Wiley: New York, 1977.

(24) Naff, W. T.; Cooper, C. D.; Compton, R. N. *J. Chem. Phys.* **1968**, *49*, 2784.

(25) Lifshitz, C.; Peers, A. M.; Grajower, R.; Weiss, M. *J. Chem. Phys.* **1970**, *53*, 4605.

(26) Christophorou, L. G. *Adv. Electron. Electron Phys.* **1978**, *46*, 55.

(27) Süzer, S.; Illenberger, E.; Baumgärtel, H. *Org. Mass Spectrom.* **1984**, *19*, 292.

(28) Fenzlaff, M.; Gerhard, R.; Illenberger, E. *J. Chem. Phys.* **1988**, *88*, 149.

(29) Tobita, S.; Meinke, M.; Illenberger, E.; Christophorou, L. G.; Baumgärtel, H.; Leach, S. *Chem. Phys.* **1992**, *161*, 501.

(30) Foster, M. S.; Beauchamp, J. L. *Chem. Phys. Lett.* **1975**, *31*, 482.

(31) Drzaic, P. S.; Brauman, J. I. *J. Am. Chem. Soc.* **1982**, *104*, 13.

(32) Knapp, M.; Echt, O.; Kreisle, D.; Recknagel, E. *J. Phys. Chem.* **1987**, *91*, 2601.

(33) Landmann, U.; Barnett, R. N.; Cleveland, C. L.; Scharf, D.; Jortner, J. *J. Phys. Chem.* **1987**, *91*, 4890.

(34) Haberland, H. In *The Chemical Physics of Atomic and Molecular Clusters*; Scoles, G., Ed.; North Holland: Amsterdam, 1990.

(35) Coe, J. V.; Lee, G. H.; Eaton, J. G.; Arnold, S. T.; Sarkas, H. W.; Bowen, K. H.; Ludewigt, C.; Haberland, H. *J. Chem. Phys.* **1990**, *92*, 3980.

(36) Lepoutre, G. *J. Phys. Chem.* **1984**, *88*, 3699.

(37) Sambe, H.; Ramaker, D. E. *Chem. Phys. Lett.* **1987**, *139*, 386.

(38) Oster, T.; Kühn, A.; Illenberger, E. *Int. J. Mass Spectrom. Ion Processes* **1989**, *89*, 1.

(39) Heni, M.; Illenberger, E. *Chem. Phys. Lett.* **1986**, *131*, 314.

(40) Illenberger, E. *Ber. Bunsen-Ges. Phys. Chem.* **1982**, *86*, 252.

(41) Klots, C. E.; Compton, R. N. *J. Chem. Phys.* **1977**, *67*, 1779.

(42) Klots, C. E.; Compton, R. N. *J. Chem. Phys.* **1978**, *69*, 1636.

(43) Klots, C. E.; Compton, R. N. *J. Chem. Phys.* **1978**, *69*, 1644.

(44) Klots, C. E.; Compton, R. N. *Chem. Phys. Lett.* **1980**, *73*, 589.

(45) Klots, C. E. *Radiat. Phys. Chem.* **1982**, *20*, 51.

(46) Klots, C. E. *J. Chem. Phys.* **1979**, *71*, 4172.

(47) Märk, T. D. *Int. J. Mass Spectrom. Ion Processes* **1991**, *107*, 143.

(48) Märk, T. D.; Leiter, K.; Ritter, W.; Stamatovic, A. *Phys. Rev. Lett.* **1985**, *55*, 2559.

(49) Märk, T. D.; Leiter, K.; Ritter, W.; Stamatovic, A. *Int. J. Mass Spectrom. Ion Processes* **1986**, *74*, 265.

(50) Walder, G.; Margreiter, D.; Winkler, C.; Stamatovic, A.; Herman, Z.; Märk, T. D. *J. Chem. Soc. Faraday Trans.* **1990**, *86*, 2395.

(51) Walder, G.; Margreiter, D.; Winkler, C.; Grill, V.; Rauth, T.; Scheier, P.; Stamatovic, A.; Herman, Z.; Foltin, M.; Märk, T. D. *Z. Phys. D* **1991**, *20*, 201.

(52) Märk, T. D.; Scheier, P.; Stamatovic, A. *Chem. Phys. Lett.* **1987**, *136*, 177.

(53) Stamatovic, A.; Scheier, P.; Märk, T. D. *Z. Phys. D* **1987**, *6*, 351.

(54) Märk, T. D.; Stamatovic, A.; Scheier, P. *Z. Phys. D* **1989**, *12*, 303.

(55) Stamatovic, A.; Scheier, P.; Märk, T. D. *J. Chem. Phys.* **1988**, *88*, 6884.

(56) Stamatovic, A.; Leiter, K.; Ritter, W.; Stephan, K.; Märk, T. D. *J. Chem. Phys.* **1985**, *83*, 2942.

(57) Stamatovic, A.; Stephan, K.; Märk, T. D. *Int. J. Mass Spectrom. Ion Processes* **1985**, *63*, 37.

(58) Knapp, M.; Echt, O.; Kreisle, D.; Recknagel, E. *J. Chem. Phys.* **1986**, *85*, 636.

(59) Knapp, M.; Kreisle, D.; Echt, O.; Sattler, K.; Recknagel, E. *Surf. Sci.* **1985**, *156*, 313.

(60) Knapp, M.; Echt, O.; Kreisle, D.; Märk, T. D.; Recknagel, E. *Chem. Phys. Lett.* **1986**, *126*, 225.

(61) Echt, O.; Knapp, M.; Schwarz, C.; Recknagel, E. In ref 3.

(62) Vostrikov, A. A.; Dubov, D. Yu.; Predtechenskii, M. R. *Sov. Phys. Tech. Phys.* **1986**, *31*, 825.

(63) Vostrikov, A. A.; Dubov, D. Yu.; Predtechenskii, M. R. *Sov. Phys. Tech. Phys.* **1987**, *32*, 459 and references therein.

(64) Lotter, J.; Kühn, A.; Illenberger, E. *Chem. Phys. Lett.* **1989**, *157*, 171.

(65) Kühn, A.; Illenberger, E. *J. Phys. Chem.* **1989**, *93*, 7060.

(66) Kühn, A.; Illenberger, E. *J. Chem. Phys.* **1990**, *93*, 357.

(67) Lotter, J.; Illenberger, E. *J. Phys. Chem.* **1990**, *94*, 8951.

(68) Hashemi, R.; Kühn, A.; Lotter, J.; Illenberger, E. *Ber. Bunsen-Ges. Phys. Chem.* **1990**, *94*, 1334.

(69) Hashemi, R.; Kühn, A.; Illenberger, E. *Int. J. Mass Spectrom. Ion. Processes* **1990**, *100*, 753.

(70) Hashemi, R.; Illenberger, E. *J. Phys. Chem.* **1991**, *95*, 6402.

(71) Hashemi, R.; Illenberger, E. *Chem. Phys. Lett.* **1991**, *187*, 623.

(72) De Luca, M. J.; Niu, B.; Johnson, M. A. *J. Chem. Phys.* **1988**, *88*, 5857.

(73) Haberland, H.; Langosch, H.; Schindler, H.-G.; Worsnop, D. R. *J. Phys. Chem.* **1984**, *88*, 3903.

(74) Haberland, H.; Ludewigt, C.; Schindler, H.-G.; Worsnop, D. R. *Surf. Sci.* **1985**, *156*, 157.

(75) Haberland, H.; Ludewigt, C.; Schindler, H.-G.; Worsnop, D. R. *Phys. Rev. A* **1987**, *36*, 967.

(76) Haberland, H.; Schindler, H.-G.; Worsnop, D. R. *Ber. Bunsen-Ges. Phys. Chem.* **1984**, *88*, 270.

(77) Stampfli, P.; Bennemann, K. H. *Phys. Rev. Lett.* **1987**, *58*, 2635.

(78) Haberland, H.; Kolar, T.; Reiners, T. *Phys. Rev. Lett.* **1989**, *63*, 1219.

(79) Barnett, R. N.; Landman, U.; Cleveland, C. L.; Jortner, J. *Phys. Rev. Lett.* **1987**, *59*, 811.

(80) Barnett, R. N.; Landman, U.; Cleveland, C. L.; Jortner, J. *J. Chem. Phys.* **1988**, *88*, 4421.

(81) Barnett, R. N.; Landman, U.; Cleveland, C. L.; Jortner, J. *J. Chem. Phys.* **1988**, *88*, 4429.

(82) Barnett, R. N.; Landman, U.; Cleveland, C. L.; Jortner, J. *Chem. Phys. Lett.* **1988**, *145*, 382.

(83) Mitsuke, K.; Kondow, T.; Kuchitsu, K. *J. Phys. Chem.* **1986**, *90*, 1552.

(84) Mitsuke, K.; Kondow, T.; Kuchitsu, K. *J. Phys. Chem.* **1986**, *90*, 1505.

(85) Tsakuda, T.; Kondow, T. *Chem. Phys. Lett.* **1991**, *185*, 511.

(86) Kraft, T.; Ruf, M.-W.; Hotop, H. *Z. Phys. D* **1989**, *14*, 179.

(87) Kraft, T.; Ruf, M.-W.; Hotop, H. *Z. Phys. D* **1991**, *20*, 13.

(88) Kraft, T.; Ruf, M.-W.; Hotop, H. *Z. Phys. D* **1991**, *18*, 403.

(89) Desfrancois, C.; Khelifa, N.; Schermann, J. P. *J. Chem. Phys.* **1989**, *91*, 5838.

(90) Desfrancois, C.; Khelifa, N.; Lisfi, A.; Schermann, J. P.; Eaton, J. G.; Bowen, K. H. *J. Chem. Phys.* **1991**, *95*, 7760.

(91) Kontrowitz, A.; Grey, J. *Rev. Sci. Instr.* **1951**, *22*, 328.

(92) Anderson, J. B. In *Molecular Beams and Low Density Gas Dynamics*; Wegener, P. P., Ed.; Marcel Dekker: New York, 1974.

(93) Miller, D. R. In *Atomic and Molecular Beam Methods*; Scoles, G., Ed.; Oxford University Press: Oxford, 1988; Vol. I.

(94) Anderson, J. B.; Fenn, J. B. *Phys. Fluids* **1965**, *8*, 780.

(95) Stamatovic, A.; Schulz, G. J. *Rev. Sci. Instr.* **1968**, *39*, 1752.

(96) Stamatovic, A.; Schulz, G. J. *Rev. Sci. Instr.* **1970**, *41*, 423.

(97) Illenberger, E. *Chem. Phys. Lett.* **1981**, *80*, 153.

(98) Illenberger, E. *Ber. Bunsen-Ges. Phys. Chem.* **1982**, *86*, 247.

(99) Massey, H. S. W. *Negative Ions*; Cambridge University Press: Cambridge, 1976.

(100) Christophorou, L. G. *Atomic and Molecular Radiation Physics*; Wiley Interscience: London, 1971.

(101) Rapp, D.; Briglia, D. D. *Chem. Phys.* **1965**, *43*, 1480.

(102) Field, D.; Mrotzek, G.; Knight, D. W.; Lunt, S.; Ziesel, J. P. *J. Phys. B* **1988**, *21*, 171.

(103) Celotta, R. J.; Bennett, R. A.; Hall, J. L.; Siegel, W.; Levine, J. *Phys. Rev. A* **1972**, *6*, 631.

(104) Spence, D.; Schulz, G. J. *Phys. Rev. A* **1972**, *5*, 724.

(105) McCorkle, D. L.; Christophorou, L. G.; Anderson, V. E. *J. Phys. B: At., Mol. Phys.* **1972**, *5*, 1211.

(106) Truby, F. K. *Phys. Rev. A* **1972**, *6*, 671.

(107) Bloch, F.; Bradbury, N. *Phys. Rev.* **1933**, *48*, 883.

(108) Chantry, P. J.; Schulz, G. J. *Phys. Rev.* **1967**, *156*, 134.

(109) O'Malley, T. F. *Phys. Rev.* **1966**, *150*, 14.

(110) Henderson, W. R.; Fite, W. L.; Brackmann, R. T. *Phys. Rev.* **1969**, *183*, 157.

(111) O'Malley, T. F. *Phys. Rev.* **1966**, *155*, 59.

(112) Sanche, L. *Phys. Rev. Lett.* **1984**, *53*, 1638.

(113) Sanche, L.; Parenteau, L.; Cloutier, P. *J. Chem. Phys.* **1989**, *91*, 2664.

(114) Sanche, L. *J. Phys. B: At., Mol. Opt. Phys.* **1990**, *23*, 1597.

(115) Sanche, L. In *Excess Electrons in Dielectric Media*; Ferradini, C., Jay-Gerin, J. J., Eds.; CRC Press: Boca Raton, 1991.

(116) Jaffke, T.; Meinke, M.; Hashemi, R.; Christophorou, L. G.; Illenberger, E. *Chem. Phys. Lett.* **1992**, *193*, 62.

(117) Belic, D. S.; Hall, R. I. *J. Phys. B* **1981**, *14*, 365.

(118) Krupenie, P. H. *J. Phys. Chem. Ref. Data* **1972**, *1*, 423.

(119) Krauss, M.; Neumann, D.; Wahl, A. C.; Das, G.; Zemke, W. *Phys. Rev. A* **1973**, *7*, 69.
(120) Sambe, H.; Ramaker, D. E. *Phys. Rev. A* **1989**, *40*, 3651.
(121) Jaffke, T.; Hashemi, R.; Christophorou, L. G.; Illenberger, E. *Z. Phys. D*, in press.
(122) Schulz, G. J.; Dowell, J. T. *Phys. Rev.* **1962**, *128*, 174.
(123) Rauth, T.; Foltin, M.; Märk, T. D. *J. Phys. Chem.* **1992**, *96*, 1528.
(124) Foltin, M.; Grill, V.; Märk, T. D. *Chem. Phys. Lett.* **1992**, *118*, 427.
(125) Jaffke, T.; Hashemi, R.; Christophorou, L. G.; Illenberger, E. *J. Phys. Chem.*, submitted for publication.
(126) Jaffke, T.; Illenberger, E. Unpublished results.
(127) Leiter, K.; Ritter, W.; Stamatovic, A.; Märk, T. D. *Int. J. Mass Spectrom. Ion Processes* **1986**, *68*, 341.
(128) Hashemi, R.; Illenberger, E. Manuscript in preparation.
(129) De Luca, M. J.; Han, C. C.; Johnson, M. A. *J. Chem. Phys.* **1990**, *93*, 268.
(130) Hiraoka, K. *J. Chem. Phys.* **1988**, *89*, 3190.
(131) Illenberger, E.; Scheunemann, H.-U.; Baumgärtel, H. *Chem. Phys.* **1979**, *37*, 21.
(132) Riley, S. J.; Wilson, K. R. *Faraday Discuss. Chem. Soc.* **1972**, *53*, 132.
(133) Krajnovich, D.; Butler, L. J.; Lee, Y. T. *J. Chem. Phys.* **1984**, *81*, 3031.
(134) Franklin, J. L. In *Gas Phase Ion Chemistry*; Bowers, M. T., Ed.; Academic Press: New York, 1976; Vol. I.
(135) Illenberger, E. *Ber. Bunsen-Ges. Phys. Chem.* **1982**, *86*, 252.
(136) Oster, T.; Hashemi, R.; Illenberger, E. Manuscript in preparation.
(137) McMillen, D. F.; Golden, D. M. *Annu. Rev. Phys. Chem.* **1982**, *33*, 493.
(138) Mead, R. D.; Stevens, A. E.; Lineberger, W. C. In *Gas Phase Ion Chemistry*; Bowers, M. T., Ed.; Academic Press: Orlando, 1984; Vol. III.
(139) Garrett, W. R. *Phys. Rev. A* **1971**, *3*, 961.
(140) Crawford, O. H. *Mol. Phy.* **1971**, *20*, 585.
(141) Mead, R. D.; Lykke, K. R.; Lineberger, W. C.; Marks, J.; Brauman, J. I. *J. Chem. Phys.* **1984**, *81*, 4883.
(142) Marks, J.; Comita, P. B.; Brauman, J. I. *J. Am. Chem. Soc.* **1985**, *107*, 3718.
(143) Marks, J.; Brauman, J. I.; Mead, R. D.; Lykke, K. R.; Lineberger, W. C. *J. Chem. Phys.* **1988**, *88*, 6785.
(144) Jordan, K. D.; Burrow, P. B. *Acc. Chem. Res.* **1978**, *11*, 341.
(145) Heni, M.; Illenberger, E. *Int. J. Mass Spectrom. Ion Processes* **1986**, *73*, 127.
(146) Sugiura, T.; Arakawa, A. In *Proc. Int. Conf. Mass Spectrometry University of Tokyo* **1970**, 858.
(147) Stockdale, J. A.; Davis, F. J.; Compton, R. N.; Klots, C. E. *J. Chem. Phys.* **1974**, *60*, 4279.
(148) Compton, R. N. In *Photophysics and Photochemistry in the Vacuum Ultraviolet*; McGlynn, S. P., Findley, S. P., Huebner, R. H., Eds.; D. Reidel: Dordrecht; 1985.
(149) Compton, R. N.; Reinhardt, P. W.; Cooper, C. D. *J. Chem. Phys.* **1978**, *68*, 1978.
(150) Hopkinson, A. C.; Lien, M. H.; Yates, K.; Csizmadia, I. G. *Int. J. Quantum Chem.* **1977**, *12*, 355 and references therein.
(151) Chiu, N. S.; Burrow, P. D.; Jordan, K. D. *Chem. Phys. Lett.* **1979**, *68*, 121.
(152) Heni, M.; Illenberger, E.; Baumgärtel, H.; Süzer, S. *Chem. Phys. Lett.* **1984**, *87*, 244.
(153) Heni, M.; Illenberger, E. *J. Electron Spectrosc. Relat. Phenom.* **1986**, *41*, 453.
(154) Paddon-Row, M. N.; Rondan, N. G.; Houk, K. N.; Jordan, K. D. *J. Am. Chem. Soc.* **1982**, *104*, 1143.
(155) Fenzlaff, M.; Illenberger, E. *Chem. Phys.* **1989**, *136*, 443.
(156) Hashemi, R. Diplomarbeit, Freie Universität Berlin, 1989.
(157) Echt, O.; Knapp, M.; Schwarz, C.; Recknagel, E. In ref 3.
(158) Melton, C. E. *J. Chem. Phys.* **1972**, *57*, 4218.
(159) Jungen, M.; Vogt, J.; Staemmler, V. *Chem. Phys.* **1979**, *37*, 49.
(160) Belic, D. S.; Landau, M.; Hall, R. I. *J. Phys. B* **1981**, *14*, 175.
(161) Moore, C. E. Atomic Energy Levels; US Dept. Commerce NSRDS-NBS35: Washington, DC, 1971.
(162) Rühl, E.; Jefferson, A.; Vaida, V. *J. Phys. Chem.* **1990**, *94*, 2990.
(163) Cox, R. A.; Hagmann, G. D. *Nature* **1988**, *332*, 796.
(164) Wecker, D.; Christodoulides, A. A.; Schindler, R. N. *Int. J. Mass Spectrom. Ion Phys.* **1981**, *38*, 391.
(165) Lee, L. C.; Smith, G. P.; Moseley, J. T.; Cosby, P. C.; Guest, J. A. *J. Chem. Phys.* **1979**, *70*, 3237.
(166) Gilles, M. K.; Lineberger, W. C. Private communication.
(167) Ertl, G.; Küppers, J. *Low Energy Electrons and Surface Chemistry*; VCH Verlagsgesellschaft: Weinheim, 1985.
(168) Willis, R. F.; Ed. *Vibrational Spectroscopy of Adsorbates*; Springer Verlag: Berlin, 1990.
(169) Christmann, K. *Introduction to Surface Physical Chemistry. Topics in Physical Chemistry*; Steinkopff: Darmstadt, 1991; Vol. I.
(170) Avouris, P.; Walkup, R. E. *Annu. Rev. Phys. Chem.* **1989**, *40*, 173.
(171) Tolk, N. H., Traum, M. M., Tully, J. C., Madey, T. E., Eds. *Desorption Induced by Electronic Transitions, DIET I*; Springer: Berlin, 1983.
(172) Brenig, W., Menzel, D., Eds. *Desorption Induced by Electronic Transitions, DIET II*; Springer: Berlin, 1985.
(173) Stulen, R. H., Knotek, M. L., Eds. *Desorption Induced by Electronic Transitions, DIET III*; Springer: Berlin, 1988.
(174) Betz, G., Varga, P., Eds. *Desorption Induced by Electronic Transitions, DIET IV*; Springer: Berlin, 1990.
(175) Palmer, R. E.; Rous, P. J. *Rev. Mod. Phys.* **1992**, *64*, 383.
(176) Sanche, L.; Parenteau, L. *J. Vac. Sci., Technol. A* **1986**, *4*, 1240.
(177) Azria, R.; Parenteau, L.; Sanche, L. *J. Chem. Phys.* **1987**, *87*, 2292.
(178) Rowntree, P.; Parenteau, L.; Sanche, L. *Chem. Phys. Lett.* **1991**, *182*, 479.
(179) Rowntree, P.; Parenteau, L.; Sanche, L. *J. Phys. Chem.* **1991**, *95*, 4902.
(180) Ingolfsson, O.; Meinke, M.; Illenberger, E. Manuscript in preparation.
(181) Verhaart, G. J.; van der Hart, W. J.; Brongersma, H. H. *Chem. Phys. Lett.* **1978**, *34*, 161.
(182) Huebner, R. H.; Bushnell, D. L., Jr.; Celotta, R. J.; Mielczarek, S. R.; Kuyatt, C. E. *Nature* **1975**, *257*, 376.
(183) Zetzsch, C.; Stuhl, F. *Ber. Bunsen-Ges. Phys. Chem.* **1977**, *81*, 437.
(184) Buck, U.; Meyer, H. *Phys. Rev. Lett.* **1984**, *52*, 109.
(185) Buck, U. *J. Phys. Chem.* **1988**, *92*, 1023.
(186) Buck, U.; Huisken, F.; Lauenstein, C.; Meyer, H.; Sroka, R. *J. Chem. Phys.* **1987**, *87*, 6276.
(187) Huisken, F.; Stemmler, M. *Chem. Phys.* **1989**, *132*, 351.
(188) Huisken, F. Habilitationsschrift, Max-Planck-Institut für Strömungsforschung, Göttingen, Bericht 2, 1990.
(189) Bonačić-Koutecký, V.; Fantucci, P.; Koutecký, J. *Chem. Rev.* **1991**, *91*, 1035.
(190) Böhm, H. J.; Ahlrichs, R.; Scharf, P.; Schiffer, H. *J. Chem. Phys.* **1984**, *81*, 1389.
(191) Christophorou, L. G. In *Proceedings 20th International Conference on Ionization Phenomena in Gases*; Il Cioco, Italy, 1991, in press.
(192) Christophorou, L. G.; Hunter, S. R.; Pinnaduwage, L. A.; Carter, J. G.; Christodoulides, A. A.; Spyrou, S. M. *Phys. Rev. Lett.* **1987**, *58*, 1316.
(193) Pinnaduwage, L. A.; Christophorou, L. G. *Chem. Phys. Lett.* **1991**, *186*, 4.